# What prevents outgassing of methane to the atmosphere in Lake Tanganyika?

Edith Durisch Kaiser,[1,2] Martin Schmid,[2] Frank Peeters,[3] Rolf Kipfer,[1,4,5] Christian Dinkel,[2] Torsten Diem,[2] Carsten J. Schubert,[2] and Bernhard Wehrli[1,2]

Received 11 February 2011; revised 4 March 2011; accepted 10 March 2011; published 16 June 2011.

[1] Tropical East African Lake Tanganyika hosts the Earth's largest anoxic freshwater body. The entire water column holds over 23 Tg of the potent greenhouse gas methane ($CH_4$). Methane is formed under sulphate poor conditions via carbon dioxide reduction or fermentation from detritus and relict sediment organic matter. Permanent density stratification supports an accumulation of $CH_4$ below the permanent oxycline. Despite $CH_4$ significance for global climate, anaerobic microbial consumption of $CH_4$ in freshwater is poorly understood. Here we provide evidence for intense methanotrophic activity not only in the oxic but also in the anoxic part of the water column of Lake Tanganyika. We measured $CH_4$, $^{13}C$ of dissolved $CH_4$, dissolved oxygen ($O_2$), sulphate ($SO_4^{2-}$), sulphide ($HS^-$) and the transient tracers chlorofluorocarbon 12 (CFC 12) and tritium ($^3H$). A basic one dimensional model, which considers vertical transport and biogeochemical fluxes and transformations, was used to interpret the vertical distribution of these substances. The results suggest that the anaerobic oxidation of $CH_4$ is an important mechanism limiting $CH_4$ to the anoxic zone of Lake Tanganyika. The important role of the anaerobic oxidation for $CH_4$ concentrations is further supported by high abundances (up to ~33% of total DAPI stained cells) of single living archaea, identified by fluorescence in situ hybridization.

**Citation:** Durisch-Kaiser, E., M. Schmid, F. Peeters, R. Kipfer, C. Dinkel, T. Diem, C. J. Schubert, and B. Wehrli (2011), What prevents outgassing of methane to the atmosphere in Lake Tanganyika?, *J. Geophys. Res.*, *116*, G02022, doi:10.1029/2010JG001323.

## 1. Introduction

[2] East African tropical lakes store approximately one quarter of the Earth's freshwater [*Bootsma and Hecky*, 2003]. Although they bear large amounts of the greenhouse gases $CO_2$ and $CH_4$ in their water bodies [*Deuser et al.*, 1973; *Rudd*, 1980; *Schmid et al.*, 2005], their contribution to the natural source of $CH_4$ to the atmosphere is to date unknown. Furthermore, there is growing evidence that lakes may represent significant sources of greenhouse gases and may dominate total natural $CH_4$ emissions [*Bastviken et al.*, 2004]. However, quantification is often difficult, due to spatially and temporally variable emission rates [*International Panel on Climate Control*, 2007; *Van der Nat and Middelburg*, 2000] and pathways [*Bastviken et al.*, 2004].

[3] In the ocean, only little $CH_4$ ever escapes to the atmosphere. Most $CH_4$ is scavenged by anaerobic microbial oxidation according to $CH_4 + SO_4^{2-} \rightarrow HCO_3^- + HS^- + H_2O$ [*Valentine and Reeburgh*, 2000]. Archaeal groups in association with sulphate-reducing bacteria were shown to mediate this process. Most of these marine archaea are related to the Methanosarcinales [*Boetius et al.*, 2000; *Michaelis et al.*, 2002; *Schubert et al.*, 2006] and are associated with sulphate-reducing bacteria, widely linked to the *Desulfosarcina/Desulfococcus* cluster (Deltaproteobacteria). For lacustrine systems only a small suite of studies exist, which prove the occurrence of anaerobic oxidation of $CH_4$ [e.g., *Iversen and Jorgensen*, 1985; *Panganiban et al.*, 1979; *Smemo and Yavitt*, 2007]. To date only two mechanisms other than the one coupled to sulphate reduction are known, namely manganese and iron reduction and denitrification [*Beal et al.*, 2009; *Raghoebarsing et al.*, 2006]. These mechanisms were reported from incubations under laboratory conditions or from seep sediment and have not yet been confirmed to occur in lakes. Conditions for anaerobic oxidation of $CH_4$ are less favorable in freshwater systems, because sulphate and dissolved metal concentrations are generally low and easily become the limiting factor.

[1] Institute of Biogeochemistry and Pollutant Dynamics, ETH, Zurich, Switzerland.
[2] Eawag, Swiss Federal Institute of Aquatic Science and Technology, Kastanienbaum, Switzerland.
[3] Limnological Institute, Department of Biology, University of Konstanz, Konstanz, Germany.
[4] Eawag, Swiss Federal Institute of Aquatic Science and Technology, Dübendorf, Switzerland.
[5] Institute of Isotope Geology and Mineral Resources, ETH, Zurich, Switzerland.


0148 0227/11/2010JG001323

[4] The oligotrophic Lake Tanganyika is a lacustrine system which is located in the African Rift Valley and seems to be well suited for a biogeochemical study of the anaerobic oxidation of $CH_4$. This lake contains the largest anoxic freshwater body in the world, storing approximately 23 Tg of $CH_4$ gas below a permanent thermal stratification [*Hecky*, 1991]. For comparison, ~90 Tg of $CH_4$ are stored in the Black Sea, the world's largest marine anoxic basin [*Reeburgh et al.*, 1991]. Furthermore, water column sulphate concentrations are substantial and allow the formation of a chemically appropriate environment for the anaerobic oxidation of $CH_4$. In Lake Tanganyika, mixing processes and currents have intensively been investigated in the surface waters [*Naithani et al.*, 2007; *Gourgue et al.*, 2007a; *Podsetchine et al.*, 1999]. Deep water renewal and vertical transport in the hypolimnion, however, have not been investigated although these processes are important for understanding the vertical distribution of dissolved substances.

[5] In the present study, the factors controlling $CH_4$ concentrations and oxidation in Lake Tanganyika were investigated by using a one-dimensional vertical advection-diffusion reaction model. Our hypothesis is that the anaerobic oxidation of $CH_4$ essentially controls $CH_4$ concentrations in stratified lakes that contain large bodies of anoxic water and sufficient amounts of sulphate, like Lake Tanganyika. The model was applied to evaluate the major transport processes occurring in the thermocline and anoxic deep water body of Lake Tanganyika. Advective deep water renewal and turbulent mixing were estimated by inverse simulation of temperature, $^3H$ and CFC-12 concentrations, similar to an earlier study in Lake Baikal [*Peeters et al.*, 2000]. The model was further used to outline the relevance of turbulent diffusion for vertical $CH_4$, $O_2$, and $SO_4^{2-}$ transport and depletion. Model results were compared with the stable C isotopic composition of dissolved $CH_4$ and the abundance of archaea and aerobic methanotrophs with depth. Overall, these data provide evidence that the anaerobic oxidation of $CH_4$ is an important mechanism controlling the removal of $CH_4$ from the water column.

## 2. Methods

### 2.1. Sampling and Analysis

[6] Water column samples were taken for geochemical and microbiological investigations at station 1 in the northern basin and at station 2 in the southern basin (Figure 1) from aboard the R/V *Maman Benita*. Geochemical samples were collected in July 2001, 2002, and 2003, i.e., during dry monsoonal winters, and in January 2004, i.e., during wet summer, and microbiological samples were collected in July 2003 and in January 2004. Previous to sampling, vertical profiles of conductivity and temperature were recorded at both stations. Subsequently, water samples were collected with Niskin bottles.

[7] For measuring $CH_4$ concentrations and stable carbon (C) isotopic ratios, water was filled into 120 mL serum bottles, poisoned with 5 mL NaOH or 50 $\mu$L of 50 mM $HgCl_2$ solution, respectively, and stored gas tight at 5°C. A 20 mL helium headspace was introduced and the samples equilibrated at 30°C for 4 h. Quantification of $CH_4$ was accomplished by injecting 200 $\mu$L of headspace from the serum vials into a Carlo Erba HRGC 5160 gas chromatograph equipped with a J&W GSQ column (30 m × 0.53 mm). Injection temperature was 70°C, FID temperature was 200°C, and the oven temperature was held at 40°C.

[8] The $\delta^{13}C$ signature of dissolved $CH_4$ was measured on an Isoprime isotope ratio mass spectrometer linked to a Trace Gas Preconcentrator (GV Instruments). The oxidation of $CH_4$ to $CO_2$ was performed by copper oxide (CuO) at 950°C. Isotopic compositions are reported in $\delta$ notation relative to the PeeDee Belemnite (VPDB) (Vienna, IAOA), determined by comparison with a 1% $CH_4$ lab standard of known isotopic composition relative to the VPDB standard. The reproducibility of analysis is ±0.8‰, and for $CH_4$ concentrations <1 $\mu$M it is ~2‰.

[9] Water for dissolved oxygen analyses was filled without any bubbles in Winkler flasks and for ammonium, nitrate, sulphate, and sulphide analyses in muffled 100 mL glass bottles. All samples were immediately measured aboard ship. Dissolved oxygen concentrations were measured using the Winkler titration method [*Grasshof*, 1983]. Ammonium, nitrate, sulphate, and sulphide concentrations were determined colorimetrically [*DEW*, 2004].

[10] For measuring bacterial abundance and investigating the microbial consortium by fluorescence in situ Hybridization (FISH) water was collected in muffled 50 mL glass bottles and killed with formaldehyde (2%). Preserved water samples (50 mL) were filtered using polycarbonate filters (0.2 $\mu$m pore size, 25 mm diameter, Millipore) and stored frozen at −20°C. Cell abundance was determined by epifluorescence microscopy (Zeiss Axioscope HBO50, 1000 magnification) of DAPI-stained cells [*Porter and Feig*, 1980]. FISH was performed on the filters [*Pernthaler et al.*, 2002], using CY3- and fluorescein-labeled 16SrRNA-targeted oligonucleotide probes (MWG Biotech AG, Switzerland): ARCH915 (5′-GTGCTCCCCCGCCAATTCCT-3′) [*Amann et al.*, 1990; *Pernthaler et al.*, 2002], type I (M□84/M□705: 3′-AGCCCGCGACTGCTCACC-5′/ 3′-CTAGACTTCCTTGTGGTC-5′) and type II (M□450: 3′-CTATTACTGCCATGGACCTA-5′) methanotrophs [*Eller et al.*, 2001]. After testing for their specificity at ~60% v/v formamide, probes for archaea were hybridized at 40% and for bacteria at 20% formamide.

[11] The transient tracers $^3H$ and CFC-12 were sampled on a previous cruise in September 1998. Water samples were collected with Niskin bottles in the southern basin at station 2. The water was filled into copper tubes and locked gas tight. Tritium concentrations were determined by measuring the increase in helium concentration in previously degassed samples using mass spectrometry [*Beyerle et al.*, 2000]. Concentrations of CFC-12 were measured with a gas chromatograph (Shimadzu GC-14 A) equipped with an electron capture detector and following the technique of *Hofer and Imboden* [1998]. The error in concentrations (at the 1 $\sigma$ level) were estimated to be ±0.1 TU for $^3H$ (1 TU = $0.2488 \times 10^{-14}$ mL STP $g^{-1}$) and ±5% for CFC-12.

### 2.2. Model Setup

[12] A one-dimensional vertical advection-diffusion-reaction model was implemented using the lake module of the software AQUASIM 2.1 [*Reichert*, 1994, 1998], which was developed to simulate various aquatic systems, like

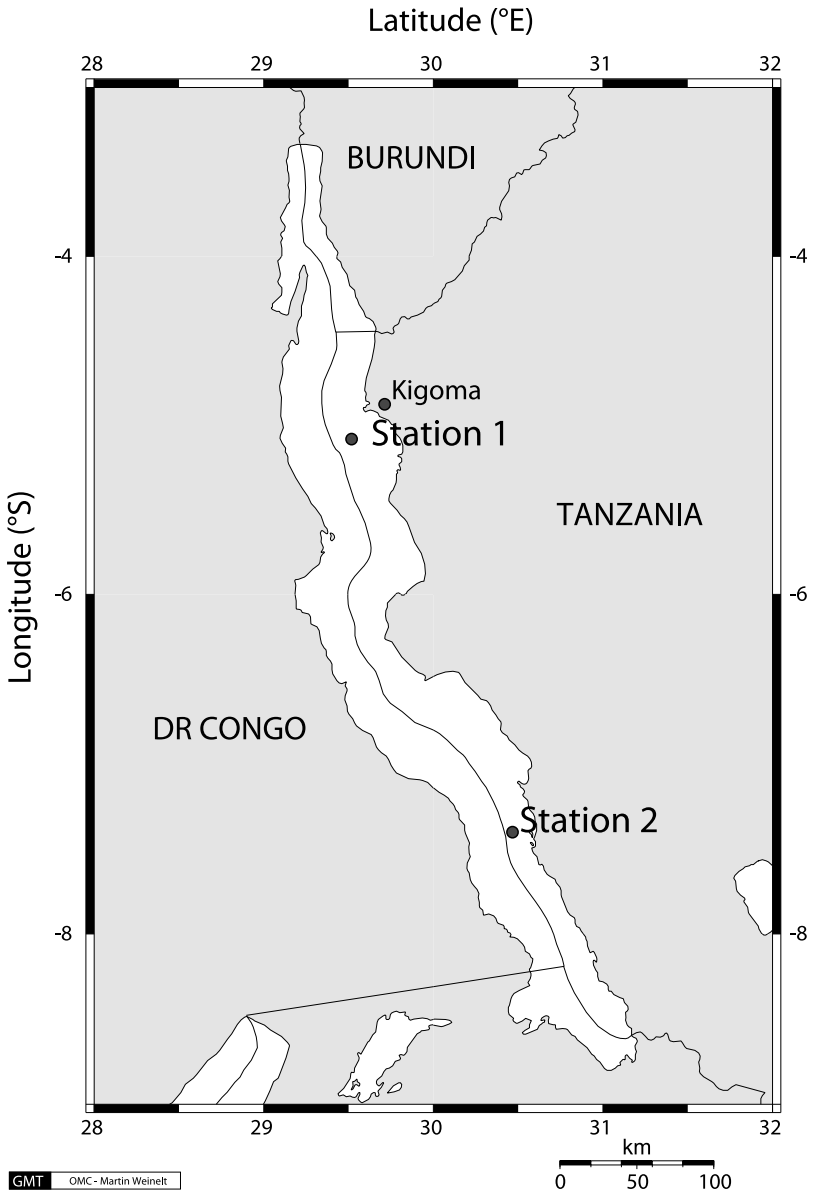


**Figure 1.** Map of Lake Tanganyika. Station 1 (5°05′S, 29°31′E, 1100 m water depth) is located in the northern basin (max. depth of 1310 m) and station 2 (7°24′S, 30°28′E, 1300 m water depth) in the southern basin (maximum depth of 1450 m). The map was created by using online map creation (OMC) by M. Weinelt (http://www.planiglobe.com/omc_set.html).

wastewater treatment plants, rivers, and particularly lakes [e.g., *Peeters et al.*, 2000; *Omlin et al.*, 2001; *Schmid et al.*, 2006; *Matzinger et al.*, 2007]. The software comprises tools for parameter estimation and sensitivity analysis. Partial differential equations for the processes included are solved by discretization of spatial derivatives, and subsequent implicit integration of the remaining system of coupled ordinary differential equations with variable time steps and variable integration order [*Petzold*, 1983]. Vertical transport processes in the model include turbulent diffusivity which varies as a function of depth and advective transport caused by lateral inflows (i.e., deep water renewal). Masses of dissolved substances are conserved. A one-dimensional vertical grid with a resolution of 5 m was used for the model.

[13] The area of Lake Tanganyika, as a function of depth, was derived from an xyz data set produced by E. Deleersnijder (personal communication, 2007) based on the bathymetric map by *Capart* [1949]. The surface area is 32900 $km^2$. The water column was divided into the mixed surface layer (0–90 m, volume 2750 $km^3$), the thermocline (90–300 m, volume 5260 $km^3$), and the deep water (below 300 m, volume 11300 $km^3$). The three basins of Lake Tanganyika (northern, intermediate, and southern) are separated by sills of an approximate depth of 700 m [*Coulter and Tiercelin*, 1991]. Although the simulation of the lake as a

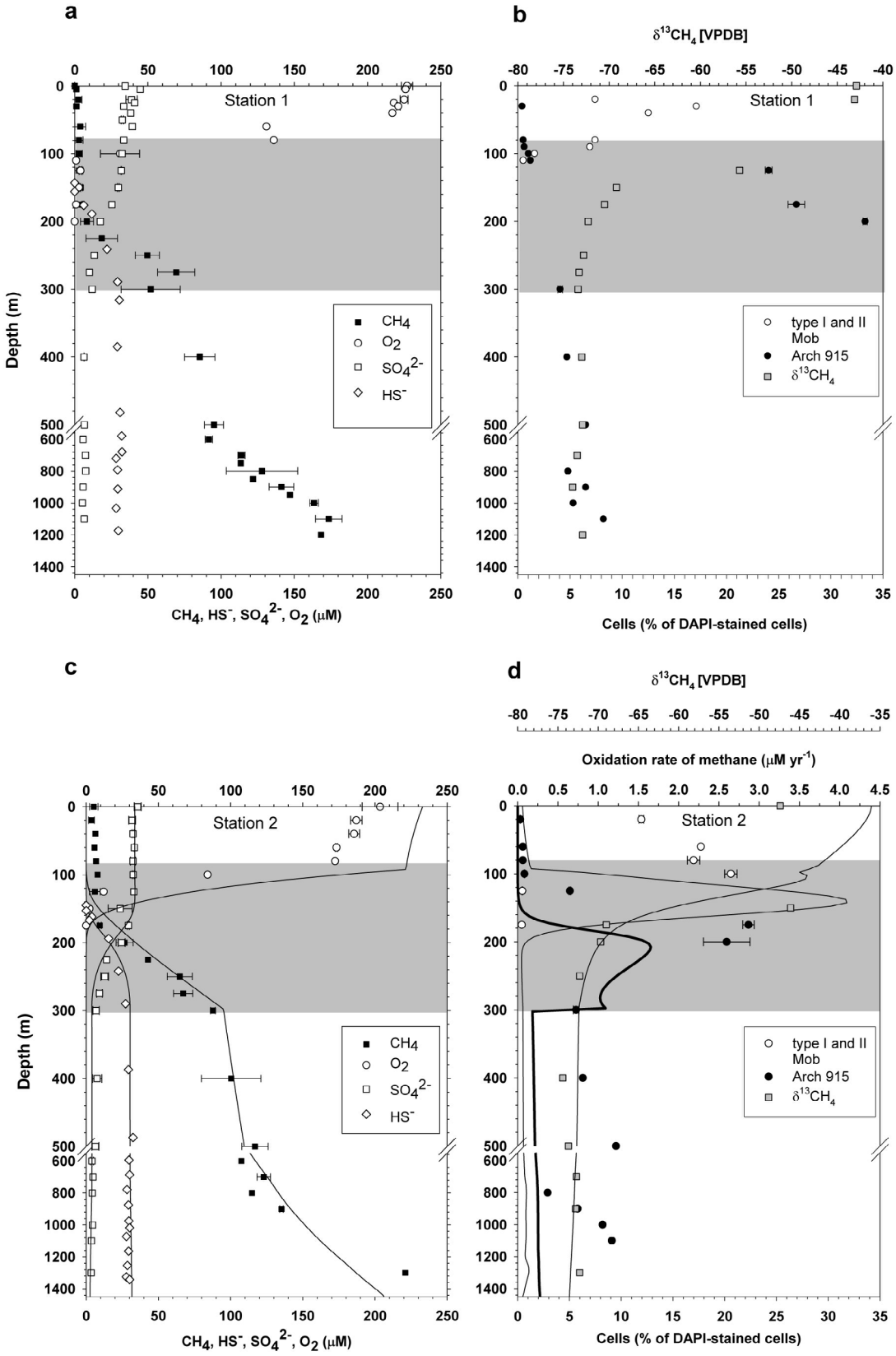
a
Station 1
Depth (m)
CH4
O2
SO4 2-
HS-
CH4, HS-, SO4 2-, O2 (μM)
b
δ13CH4 [VPDB]
Station 1
type I and II Mob
Arch 915
δ13CH4
Cells (% of DAPI-stained cells)
c
Station 2
Depth (m)
CH4
O2
SO4 2-
HS-
CH4, HS-, SO4 2-, O2 (μM)
d
δ13CH4 [VPDB]
Oxidation rate of methane (μM yr-1)
Station 2
type I and II Mob
Arch 915
δ13CH4
Cells (% of DAPI-stained cells)

**Figure 2**

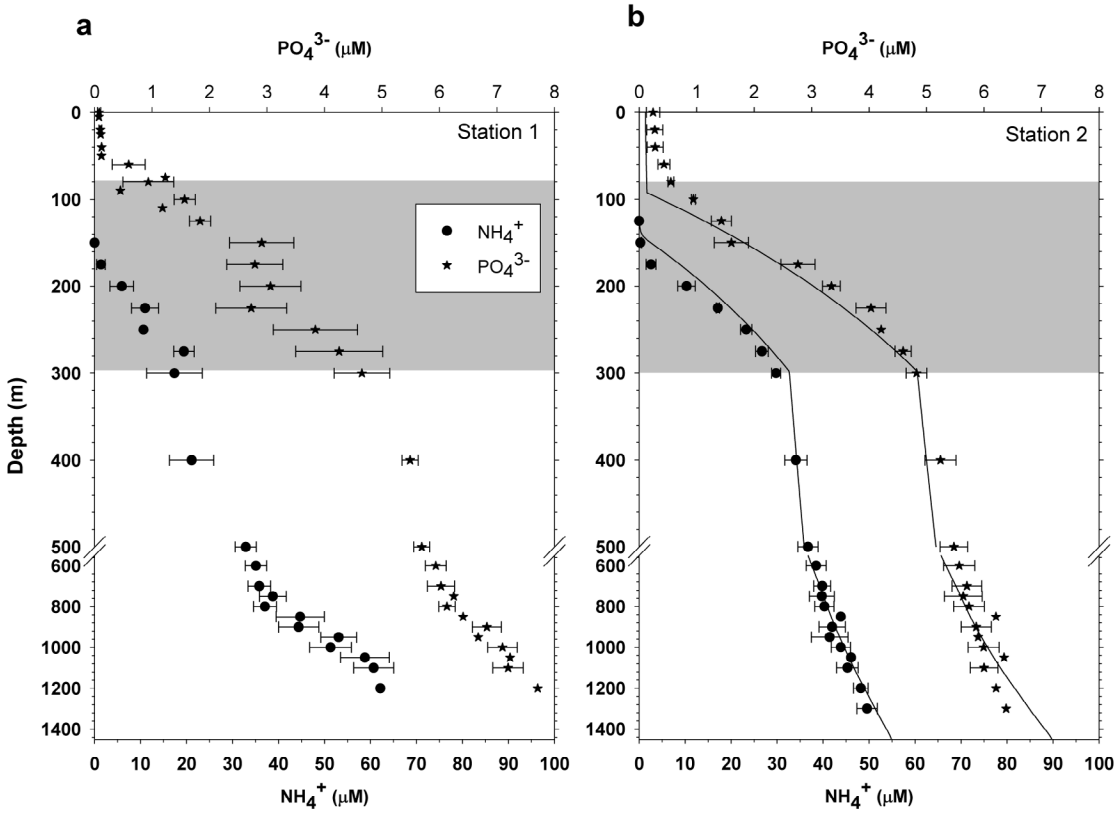


**Figure 3.** Observed (symbols) and simulated (solid line) $NH_4^+$ and $PO_4^3$ concentrations in the water column of the (a) northern basin and (b) southern basin.

single basin represents a simplification, we argue that the major processes of interest were observed above 700 m depth. The water column was divided into the mixed surface layer (0–90 m), the thermocline (90–300 m), and the deep water (below 300 m). The thickness of the surface layer was defined by the typical maximum depth reached by seasonal mixing during the dry season [*Gourgue et al.*, 2007b]. The depth separating the thermocline and the deep water (300 m) was chosen based on observed profiles of temperature and dissolved constituents from the southern basin (Figures 2, 3, and 4).

[14] Simulations were started in the year 1913 und run until 2004, with a variable time step chosen by the integration algorithm of AQUASIM 2.1, which is based on stability criteria for the solution. The maximum time step was set to 0.1 years. Table 1 lists values and source references for the external forcing and the major model parameters. Air temperature and humidity values typical for the dry season (winter) were chosen, because they are representative for the time of the year when the surface layer is mixed. An additional simulation with seasonally varying forcing was run within the 'sensitivity analysis' (see below).

[15] Average concentrations of $CH_4$, $O_2$, $SO_4^2$ , HS , $PO_4^3$ , and $NH_4^+$, and the stable C isotopic ratio of dissolved $CH_4$ ($\delta^{13}CH_4$) in the southern basin (Figures 2c and 3b) represented initial conditions in the lake's water column. For HS , the profile measured by *Edmond et al.* [1993] in the southern basin was used, since our own measurements scattered considerably. Observations from the northern basin were not used for simulations, but are shown in some figures for comparison (Figures 2a and 3a). Steady state conditions were assumed for all tracers in Lake Tanganyika except for temperature and the transient tracers CFC-12 and $^3H$. Temperature has been increasing in Lake Tanganyika during the last 100 years. The vertical profile from *Stappers* [1913], as presented by *Verburg and Hecky* [2009], was used to represent the initial condition (Figure 4). All observed in situ temperatures were converted to potential

**Figure 2.** Chemical zoning and distribution of methanotrophy indicators (Figures 2a and 2c) and of cells and oxidation rates of methane (Figures 2b and d) across the Lake Tanganyika thermocline and anoxic regime at (a and b) station 1 and (c and d) station 2. Average (±2 SE) concentrations of $CH_4$, $O_2$, and HS from 2001, 2002, 2003, and 2004, and stable C isotope ratios of dissolved $CH_4$ ($\delta^{13}C$[VPDB]) from 2004 are presented. Concentrations of HS were taken from *Edmond et al.* [1993] because our data scattered considerably. Solid lines (Figure 2c) represent modeled data. Average percentages (±% mean deviation) of archaea (ARCH915) and type I and II methanotrophs (Mob) of DAPI-stained cells from 2003 and 2004 are shown. The solid thin line (Figure 2d) represents model-derived aerobic and the solid bold line (Figure 2d) model-derived anaerobic oxidation rates of methane. The thermocline zone is indicated by shading.

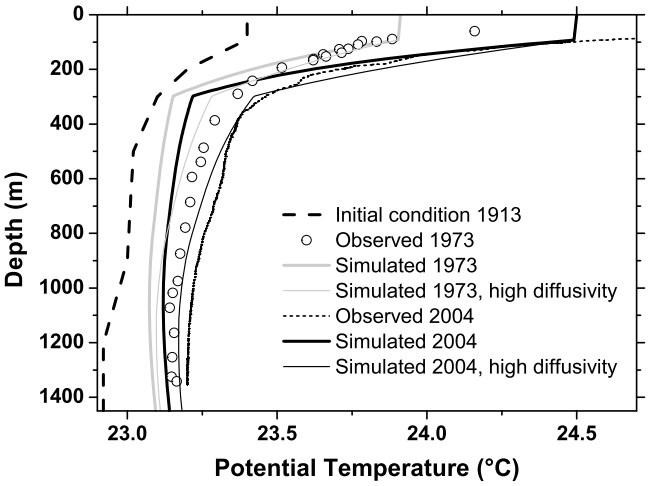


**Figure 4.** Potential temperature in the water column of Lake Tanganyika: initial condition (year 1913) and observed and simulated values for the years 1973 and 2004 with standard diffusivity and diffusivity in the thermocline increased by a factor of 2 from $1.0 \times 10^{-5}$ m$^2$ s$^{-1}$ to $2.0 \times 10^{-5}$ m$^2$ s$^{-1}$. The simulations correspond to temperature profiles during seasonal mixing and therefore are not expected to agree with observations in the mixolimnion.

temperatures by subtracting an average adiabatic temperature gradient of $1.75 \times 10^{-4}$ °C m$^{-1}$.

[16] Time-varying atmospheric concentrations of CFC-12 were represented by average observed concentrations from the Southern hemisphere [*Walker et al.*, 2000]. Solubility in water was calculated by using the constants of *Warner and Weiss* [1985]. The CFC-12 concentrations in riverine inflows were assumed to be in equilibrium with the atmosphere. In addition to our $^3$H data, one profile of $^3$H concentrations was available from measurements performed in the northern basin in 1973 [*Craig*, 1975]. Tritium concentrations in rain and riverine inflows were set to the average of concentrations observed at stations within the GNIP network [*International Atomic Energy Agency/World Meteorological Organization*, 2006] located nearby (Entebbe, Muguga, Makutapora, Kericho, Dar es Salaam, Ndola, Harare).

[17] Gas exchange (for CFC-12, $CH_4$, and $O_2$) between the surface of the lake and the atmosphere was calculated according to

$$F_C = v_{gas}\left(C_{equ} \quad C_{surf}\right) \tag{1}$$

The flux $F_c$ between the lake surface and the atmosphere was equal to the product of the gas exchange velocity $v_{gas}$ and the difference between the equilibrium $C_{equ}$ and the actual concentration at the surface $C_{surf}$. The gas exchange velocity for a Schmidt number of 600 ($Sc = 600$) was calculated according to equation (5) of *Cole and Caraco* [1998]. The exchange

**Table 1.** Major Model and External Forcing Parameters

| Parameter | Abbreviation | Value | Unit | Source |
|---|---|---|---|---|
| $^{13}$C fractionation factor for aerobic oxidation of $CH_4$ | $\alpha_{CH4,aer}$ | 0.98 | | *Whiticar* [1999] |
| $^{13}$C fractionation factor for anaerobic oxidation of $CH_4$ | $\alpha_{CH4,anaer}$ | 0.995 | | *Whiticar* [1999] |
| $^{13}$C fractionation factor for gas exchange at the lake surface | $\alpha_{CH4,gas}$ | 0.9992 | | *Knox et al.* [1992] |
| Vertical turbulent diffusivity in the deep water (below 300 m depth) | $K_{Z,deep}$ | $1.0 \times 10^{-4}$ | m$^2$ s$^{-1}$ | estimated parameter |
| Vertical turbulent diffusivity in the thermocline (between 90 and 300 m depth) | $K_{Z,thermo}$ | $1.0 \times 10^{-5}$ | m$^2$ s$^{-1}$ | estimated parameter |
| Vertical turbulent diffusivity in the mixolimnion | $K_{Z,mix}$ | $1.0 \times 10^{-3}$ | m$^2$ s$^{-1}$ | estimated parameter |
| Deep water renewal rate (below 90 m depth) | $Q_{deep}$ | 35 | km$^3$ yr$^{-1}$ | estimated parameter |
| Geothermal heat flux | $F_{geo}$ | 0.05 | W m$^{-2}$ | *Pollack et al.* [1993] |
| Areal release of $CH_4$ from sediment | $r_{CH4,sed}$ | 0.5 | Mol m$^{-2}$ yr$^{-1}$ | estimated parameter |
| Areal release of $NH_4$ from sediment | $r_{NH4,sed}$ | 0.09 | Mol m$^{-2}$ yr$^{-1}$ | estimated parameter |
| Areal release of $PO_4^{3-}$ from sediment | $r_{PO4,sed}$ | 0.01 | Mol m$^{-2}$ yr$^{-1}$ | estimated parameter |
| Oxidation rate of $H_2S$ with $O_2$ | $k_{Ox,H2S}$ | 0.16 | ($\mu$mol L$^{-1}$)$^{-1}$ yr$^{-1}$ | *Wang and Van Cappellen* [1996] |
| Rate of aerobic oxidation of $CH_4$ | $k_{Ox,CH4,aer}$ | 0.02 | ($\mu$mol L$^{-1}$)$^{-1}$ yr$^{-1}$ | estimated parameter |
| Rate of anaerobic oxidation of $CH_4$ in the thermocline | $k_{Ox,CH4,anaer,thermo}$ | 0.003 | ($\mu$mol L$^{-1}$)$^{-1}$ yr$^{-1}$ | estimated parameter |
| Rate of anaerobic oxidation of $CH_4$ in the deep water | $k_{Ox,CH4,anaer,deep}$ | 0.0004 | ($\mu$mol L$^{-1}$)$^{-1}$ yr$^{-1}$ | estimated parameter |
| Half saturation constant for limitation of anaerobic oxidation of $CH_4$ by $O_2$ | $K_{O2\ CH4}$ | 1 | $\mu$mol L$^{-1}$ | tentative, order of magnitude as for anammox bacteria [*Strous and Jetten*, 2004] |
| First order consumption rate of oxygen | $k_{O2}$ | 0.2 | yr$^{-1}$ | estimated parameter |
| First order consumption rate of $PO_4^{3-}$ above 40 m depth | $k_{PO4}$ | 2 | yr$^{-1}$ | estimated parameter |
| First order consumption rate of $NH_4^+$ above 150 m depth | $k_{NH4}$ | 10 | yr$^{-1}$ | arbitrary |
| Isotopic signature $\delta^{13}C$ of CH4 released from mineralization | $\delta^{13}C_{CH4,sed}$ | −75 | ‰ | estimated parameter |
| Precipitation | $Q_P$ | 35.5 | km$^3$ yr$^{-1}$ | *Branchu and Bergonzini* [2004][a] |
| Evaporation | $Q_E$ | 55.3 | km$^3$ yr$^{-1}$ | *Branchu and Bergonzini* [2004][b] |
| Inflows | $Q_P$ | 29.5 | km$^3$ yr$^{-1}$ | *Branchu and Bergonzini* [2004][c] |
| Wind speed | $v_{wind}$ | 3 | m s$^{-1}$ | *O'Reilly et al.* [2003] |
| Relative humidity during the dry season | $h_r$ | 60 | % | *Spigel and Coulter* [1996] |

[a]Other estimates are 35 km$^3$ yr$^{-1}$ [*Spigel and Coulter*, 1996] and 42.8 km$^3$ yr$^{-1}$ [*Nicholson and Yin*, 2004].
[b]Other estimates are 50 km$^3$ yr$^{-1}$ [*Spigel and Coulter*, 1996] and 56.5 km$^3$ yr$^{-1}$ [*Nicholson and Yin*, 2004].
[c]Other estimate is 18 km$^3$ yr$^{-1}$ [*Spigel and Coulter*, 1996].

**Table 2.** Geochemical Processes Included in the Model

| Process | Process Rate | Stoichiometric Coefficients | | | | | |
|---|---|---|---|---|---|---|---|
| | | $CH_4$[a] | $SO_4^{2-}$ | HS | $O_2$ | $NH_4^+$ | $PO_4^{3-}$ |
| Anaerobic decomposition of organic material[b] | $r_{CH4,sed} \times dA/dz \times (1/A)$ | 1 | | | | 0.18 | 0.02 |
| Aerobic oxidation of $CH_4$ | $k_{Ox,CH4,aer} \times [O_2] \times [CH_4]$ | −1 | | | −2 | | |
| Anaerobic oxidation of $CH_4$[c] | $k_{Ox,CH4,anaer} \times [SO_4] \times [CH_4] \times (1 - [O_2]/(K_{O2\ CH4} + [O_2]))$ | −1 | −1 | 1 | | | |
| HS oxidation | $k_{Ox,H2S} \times [HS^-] \times [O_2]$ | | 1 | −1 | −2 | | |
| $O_2$ consumption | $k_{O2} \times [O_2]$ | | | | −1 | | |
| $NH_4^+$ consumption[d] | $k_{NH4} \times [NH_4^+]$ | | | | | −1 | |
| $PO_4^{3-}$ consumption[e] | $k_{PO4} \times [PO_4^{3-}]$ | | | | | | −1 |

[a]All processes influencing $CH_4$ were separately simulated for the heavier C isotope ($^{13}CH_4$), using the fractionation factors and the isotopic signature of the $CH_4$ from organic material given in Table 1.
[b]Released from sediments proportional to sediment area, only below 90 m depth.
[c]Different reaction rate constants were used in the thermocline and in the deep water (Table 1).
[d]Only above 150 m depth, arbitrary rate with the aim of quickly removing $NH_4^+$.
[e]Only above 40 m depth, rate set to reach concentrations comparable to observations.

velocities of the different gases were corrected for the Schmidt numbers of the respective gases using

$$v_{gas} = v_{gas,600}(600/Sc)^n \quad (2)$$

with n = 2/3. The Schmidt numbers of the different gases were calculated as a function of temperature using the polynoms given by *Wanninkhof* [1992].

[18] The exchange of $^3H$ between the lake and the atmosphere was calculated using the equations given by *Imboden et al.* [1977]. The surface input of $^3H$ is given by

$$F_{3H} = E\frac{\alpha(C_{surf} \quad hC_{rain})}{1 \quad h} \quad (3)$$

in which $E$ represents the evaporation, $\alpha$ the equilibrium fractionation between water and air, $h$ the relative humidity of the air at the water surface temperature, $C_{surf}$ the concentration at the surface, and $C_{rain}$ the observed concentrations in rainwater [*Aeschbach-Hertig*, 1994; *Imboden et al.*, 1977]. Because the difference between air and surface water temperatures was generally small in Lake Tanganyika, relative humidity values from the air were regarded representative for $h$. Tritium was simulated to decay in the water column with a decay constant of 0.05626 $yr^{-1}$, corresponding to a half-life time of 12.32 years [*Lucas and Unterweger*, 2000].

[19] The vertical turbulent diffusivity in the surface layer is set to a value such that the water age, defined in the model as the time since the last contact with the lake surface, is on average 1 year in the mixolimnion. This requires a diffusivity of $1 \times 10^{-3}$ $m^2$ $s^{-1}$.

[20] In order to simulate $CH_4$ concentrations in the lake, the gas exchange process described above and the following processes were included in the model (Table 2): release of $CH_4$ from the sediment (proportional to the sediment area at each depth), aerobic and anaerobic oxidation of methane, oxidation of HS to $SO_4^{2-}$, and volumetric consumption of $O_2$. In order to keep $SO_4^{2-}$ concentrations constant in the surface layer, $SO_4^{2-}$ concentrations in the riverine inflows were set to 10 $\mu$M. This equals the average observed concentrations [*Langenberg et al.*, 2003], except for the River Ruzizi, which exhibits an average $SO_4^{2-}$ concentration of 124 $\mu$M and contributes 5.4 $km^3$ $yr^{-1}$ to the total river inflow, i.e., ~600 mmol $yr^{-1}$ more than included in the model. We conclude that there must be an additional sink of ~20 mmol $SO_4^{2-}$ $m^{-2}$ $yr^{-1}$ from the mixolimnion, which is not explicitly represented by a process in the model.

[21] The $\delta^{13}CH_4$ values were calculated based on the following assumptions: The $\delta^{13}C$ of $CH_4$ released from the sediment was estimated in order to fit the simulated $\delta^{13}C$ in the deep water to the observed values. The fractionation factors $\alpha$ were set to 0.98 (i.e., the reaction is 0.98 times as fast for $^{13}CH_4$ as for $^{12}CH_4$) for aerobic oxidation of $CH_4$ and to 0.995 for anaerobic oxidation of $CH_4$, both in the range of those cited by *Whiticar* [1999]. For gas exchange at the lake surface, a fractionation factor of 0.9992 was used [*Knox et al.*, 1992].

[22] In a first step, the model was used to estimate the relevant parameters for vertical transport (vertical turbulent diffusivities and deep water renewal rates) based on transient tracers and temperature profiles. Then, concentrations of the nutrients $NH_4^+$ and $PO_4^{3-}$ were simulated with the transport parameters obtained from the inverse fitting of the transient tracers to validate the parameterization of the transport processes. Finally, the validated transport model was extended by including biogeochemical processes, and the implications of these processes on $CH_4$ concentrations in the lake were investigated.

## 3. Results

### 3.1. Observed Water Column Concentrations of $O_2$, $CH_4$, $SO_4^{2-}$, HS, $NH_4^+$, $PO_4^{3-}$, and $\delta^{13}CH_4$ Values

[23] Average measured concentrations ($\mu$M ± standard error, SE, if n = 3) from water samples of the northern and southern basin are presented in Figures 2 and 3. In the northern basin, the deep water below ~200 m depth was permanently anoxic, and $CH_4$ concentrations were ~170 $\mu$M at 1200 m, ~8 $\mu$M at 200 m depth, and ~0.1 $\mu$M at the surface. In the southern basin, water column profiles were comparable to the deep northern basin (~220 $\mu$M at 1200 m, ~27 $\mu$M at 200 m depth, and ~5 $\mu$M at the surface) (Figures 2a and 2c). In the northern basin, the $\delta^{13}CH_4$ values were fairly homogenous below ~200 m depth (−72‰), however, within the thermocline $CH_4$ was heavier, and −43‰ at the surface. Note, the $\delta^{13}C$ of atmospheric $CH_4$ is −47‰ [*Stevens and Wahlen*, 2000]. In the southern basin, the $\delta^{13}CH_4$ value was fairly

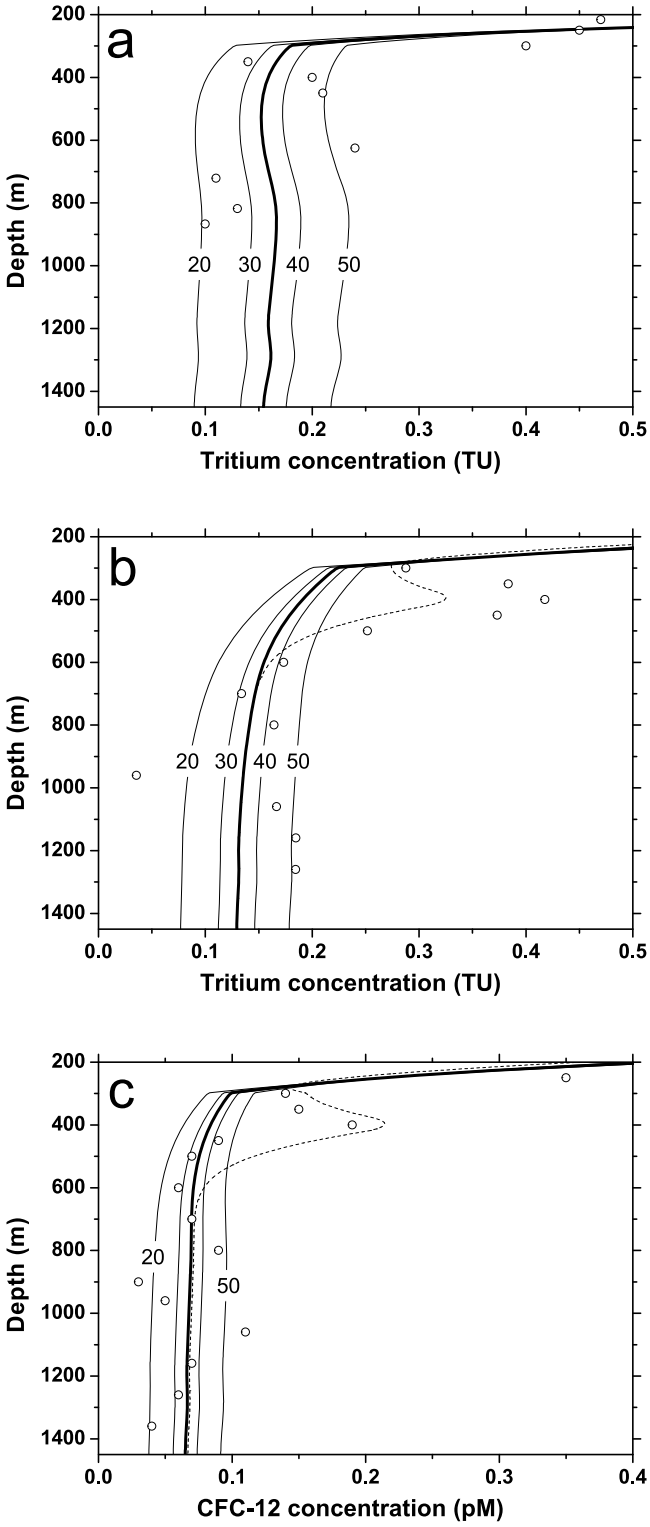


**Figure 5.** Observed concentrations (circles) in the deep water of Lake Tanganyika compared to simulations (lines) for different deep water renewal rates of (a) $^3$H in 1973, (b) $^3$H in 1998, and (c) CFC-12 in 1998. Volume flows (km$^3$ yr$^{-1}$) are indicated by numbers on the lines. The thick lines indicate the standard simulation with a flow of 35 km$^3$ yr$^{-1}$; the thin dashed lines represent a simulation with an additional surface water input of 300 km$^3$ at 400 m depth during the previous year.

homogeneous below and above the thermocline, while within it sharply shifted from −70‰ to −46‰. Sulphate, a possible electron acceptor for the anaerobic oxidation of $CH_4$, ranged between 30 and 36 $\mu$M in the surface water of both basins and showed a sharp decrease at ~200 m depth and below, while HS appeared in the thermocline and concentrations were high (>50 $\mu$M) below. However, the HS data were strongly scattered (data not shown), and therefore the data by *Edmond et al.* [1993] from the southern basin were used for model simulations. Ammonium concentrations were highest in deep water (50 to 60 $\mu$M) and the sharpest upward decrease occurred between 300 and 150 m depth in both basins (Figure 3). Similarly, $PO_4^3$ concentrations were highest in deep water (6 to 8 $\mu$M) and concentrations strongly decreased between 300 and 80 m depth in both basins.

### 3.2. Cell Abundance and FISH

[24] We detected numerous single cells from water column samples with gene probes specific for the domains archaea and bacteria using FISH. In both basins, an increase of the abundance of archaea (up to ~33% of total DAPI-stained cells in the northern basin) was identified in the thermocline (Figures 2b and 2d). The archaeal cells were well recognized by DAPI stain and probe signal. About 12 to 17% of all DAPI-stained cells within 30 to 40 m depth in the northern and 19 to 22% at 100 m depth in the southern basin were identified to belong to type I and II methanotrophs. Type I methanotrophs dominated by up to 95%.

### 3.3. Diffusivity, Temperature, and Deep Water Renewal

[25] Below 400 m depth, the transient tracers CFC-12 and $^3$H were observed at significant concentrations, with a considerable scatter, but no clear depth trend. In principle, there are two possibilities to explain these concentrations: (1) very high vertical turbulent diffusivities or (2) an advective transport of surface water to the deep water. The former contradicts both the observed gradients of other constituents in the deep water, and a first-order estimate of the diffusivity in the thermocline of $\leq 10^{-5}$ m$^2$ s$^{-1}$, which was based on the vertical density stratification and the energy input from the wind using the method described by *Wüest et al.* [2000].

[26] For this reason, the volume flow of deep water renewal in the thermocline between 90 to 350 m depth was optimized to fit the observed water column concentrations of CFC-12 and $^3$H (Figure 5). For $^3$H and CFC-12, zero concentrations were assumed as initial conditions for the year 1904. Then, the model was run until the years 1973 [*Craig*, 1975]) and 1998, when concentrations were measured.

[27] It is assumed that the deep water is formed by plunging surface water due to differential cooling in shallower areas of the lake [*Verburg and Hecky*, 2009], similar to the processes described for Lake Issyk-Kul [*Peeters et al.*, 2003]. The vertical depth distribution of the deep water new formation is unknown. Several different distributions were tested, and the most consistent results were achieved by assuming a formation rate that decreases linearly from 90 m depth to the deepest point of the lake. Least squares fitting to the observed concentrations of $^3$H (1973 and 1998) and CFC-12 (1998) below 400 m depth resulted in consistent deep water renewal rates below 90 depth of 37.4 km$^3$ yr$^{-1}$

and 32.5 $km^3$ $yr^{-1}$, respectively. In reality, the deep water renewal is a highly dynamic process and it must be assumed that both the quantity and the depth distribution vary significantly from year to year. For further calculations, a constant deep water renewal rate of 35 $km^3$ $yr^{-1}$ was assumed below 90 m depth, of which 24 $km^3$ $yr^{-1}$ are discharged below 300 m depth. Concentrations of $CH_4$, $HS^-$, $SO_4^{2-}$, $O_2$, CFC-12, and $^3H$ in the deep water inflow were set equal to concentrations at 10 m depth.

[28] The vertical temperature profiles in the thermocline follow exponential curves. This would be expected in case of a constant diffusivity combined with upwards advection driven by deep water renewal. By fitting an exponential curve to the observed profiles, the ratio of the turbulent diffusivity to the uplift velocity caused by deep water renewal rate can be estimated. The resulting diffusivity in the thermocline is $6 \times 10^{-6}$ $m^2$ $s^{-1}$, in agreement with the first-order estimate based on the method of *Wüest et al.* [2000]. The diffusivity in the thermocline can also be optimized in order to reproduce the observed temperature increase over time [*Verburg and Hecky*, 2009]. This requires several assumptions: we assumed that the water propagating downward in the deep water renewal process is slightly (0.1°C) colder than the ambient water at the depth where it intrudes and stratifies, that the geothermal heat flow corresponds to the average of the few available observations (0.5 W $m^{-2}$ [*Pollack et al.*, 1993]), and that there is no significant heating by warm springs, even though geothermal springs are entering the surface layer [*Tiercelin et al.*, 1993]. Furthermore, it was assumed that the temperature at the base of the mixolimnion has been increasing by ~1°C within a century, namely from 23.5°C in 1900 to 23.9°C in 1975 and 24.5°C in 2000. A diffusivity value on the order of $2 \times 10^{-5}$ $m^2$ $s^{-1}$ would then be required in order to supply sufficient heat to the deep water (Figure 4). Based on this evaluation, the diffusivity in the thermocline was set to $1 \times 10^{-5}$ $m^2$ $s^{-1}$. We estimate that this diffusivity should be correct within a factor of 2.

[29] The diffusivity in the deep water is less well constrained. Measured vertical profiles of $NH_4^+$ and $PO_4^{3-}$ concentrations from 1975 [*Edmond et al.*, 1993] and from 2002 to 2004 (data not shown) show very consistent gradients in the deep water, indicating that the chemical conditions in the deep water are near steady state. The average observed gradients of chemical compounds such as alkalinity, silica, $NH_4^+$ and $PO_4^{3-}$, in the deep water of the southern basin are typically by a factor of ~10 smaller compared to the thermocline. If we assume areal fluxes to be similar over depth, this indicates that the diffusivity in the deep water is about 10 times larger than in the thermocline. Hence, we tentatively set the diffusivity in the deep water to $1 \times 10^{-4}$ $m^2$ $s^{-1}$.

[30] The observed profiles of the transient tracers CFC-12 and $^3H$ show two features that cannot be explained by the simple model approach (Figure 5). In 1998, elevated concentrations were observed at around 400 m depth, which would require a large intrusion event at this depth. Based on the estimated vertical diffusivity in the deep water of the lake, the width of the peak indicates an average age of the intrusion of approximately 1 year. An additional simulation was run with an individual inflow of 300 $km^3$ of water at 400 m depth during the year 1997 and is shown for comparison in Figures 5b and 5c. Such an intrusion could explain the observed concentrations of the transient tracers. It is unclear how well the peak would have been horizontally distributed across the whole lake within one year. The observed peaks could therefore also be interpreted as a rather local signal of a smaller intrusion or as a more distant signal of an even larger event in another basin. Negative peaks at around 900 m depth may suggest an inflow of old groundwater, which has not been in contact with the atmosphere for at least 50 years.

### 3.4. Simulation of Nutrient and Oxygen Concentrations

[31] In order to examine the assumptions for mixing derived above, concentrations of $NH_4^+$ and $PO_4^{3-}$ were simulated. For both compounds it was assumed that they are released at a constant rate proportional to the sediment area at all depths. There are no data available from Lake Tanganyika to support this assumption. This would require measurements of sediment fluxes with sediment traps at different depths. However, in Lake Kivu, water column mineralization in the anoxic layer was shown to be negligible, and observed sediment fluxes were homogeneous with depth [*Pasche et al.*, 2010]. In the model, $NH_4^+$ is quickly consumed by nitrification with an arbitrary fast rate at depths <150 m in order to keep mixolimnion concentrations at very low levels, and $PO_4^{3-}$ is consumed by primary production in the mixolimnion at a first order rate of 2 $yr^{-1}$ to keep surface concentrations near typical observed levels of 0.1 $\mu$M. Areal release rates of ~0.09 mol $NH_4^+$ $m^{-2}$ $yr^{-1}$ and ~0.01 mol $PO_4^{3-}$ $m^{-2}$ $yr^{-1}$ are required to keep the concentrations constant in the deep water. Simulated concentrations agree well with observations, supporting the assumptions for mixing processes made above (Figure 3b). It should be mentioned that, assuming a C:N:P ratio of 168:19:1 [*Järvinen et al.*, 1999] of the mineralized organic matter, the release rates would correspond to a relatively low mineralization rate of ~10–20 g C $m^{-2}$ $yr^{-1}$ (comparable to that of *Ramlal et al.* [2003]). A first order volumetric oxygen consumption rate of 0.2 $yr^{-1}$ was required to reproduce the observed vertical oxygen profile.

### 3.5. Production and Oxidation of Methane

[32] The observed concentrations could best be reproduced in steady state using an areal production of 0.5 mol $CH_4$ $m^{-2}$ $yr^{-1}$ (Figure 2). The estimated ratio of C:N:P of the mineralized organic matter, assuming a production of 50% $CO_2$ and 50% $CH_4$ during anaerobic decomposition, was 100:9:1. Compared to the average composition of the seston, P is enriched by a factor of almost 2 in the mineralized organic matter. This enrichment is at least partially due to seasonal effects. During the dry season, primary production peaks while N and P are enriched in the seston compared to the annual average [*Stenuite et al.*, 2007]. Furthermore, it can be expected that a higher fraction of the freshly produced organic matter is exported from the epilimnion during the dry season than during the wet season when nutrients are more limiting and the stratification is more stable. The sedimenting and mineralized organic matter is therefore more representative of the organic matter produced during the dry season, as it has been observed using sediment traps in Lake Malawi [*Pilskaln*, 2004]. The $\delta^{13}C$ of the produced $CH_4$ was set to −75 ‰ in order to agree with the observed $\delta^{13}C$ of the $CH_4$ in deep water (Figure 2). The

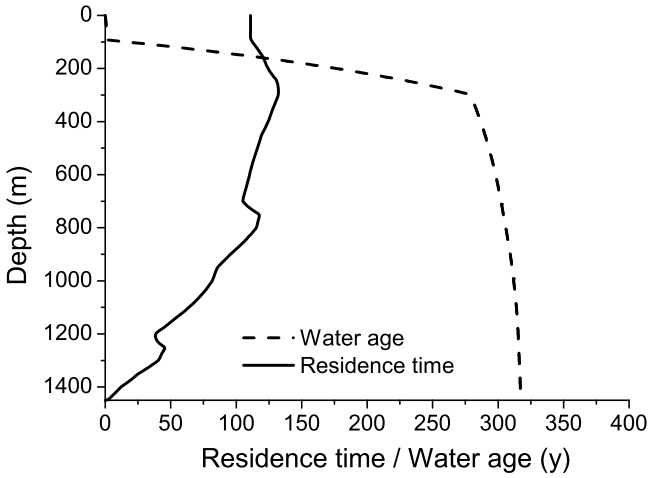


**Figure 6.** Simulated average residence time of $CH_4$ (calculated as the stock below a given depth divided by the integrated production below this depth) and water age (average time since the last contact of the water with the atmosphere at the lake surface).

$CH_4$ observed in the deep water is ~2 ‰ heavier because of the partial oxidation with $O_2$ and $SO_4^{2-}$ supplied by the deep water renewal.

[33] The rates of the aerobic and anaerobic oxidation of $CH_4$ were adjusted to fit the observed gradients of $CH_4$, $HS^-$, and $SO_4^{2-}$ with depth. It was not possible to reproduce both the gradient of $CH_4$ in the thermocline and the $SO_4^{2-}$ concentrations in the deep water with the same reaction rate for anaerobic $CH_4$ oxidation. In reality, the supply of $SO_4^{2-}$ by deep water renewal is intermittent, with varying depths and volumes of intrusions, contrary to the thermocline, where $SO_4^{2-}$ is continuously supplied from the mixolimnion by turbulent diffusion, supporting the activity of a more 'efficient' population of anaerobically oxidizing $CH_4$ cells. Therefore we used different reaction rate constants for the anaerobic oxidation of $CH_4$ in the thermocline and the deep water in the model. The reaction rate constants were estimated to 0.02 $yr^{-1}$ ($\mu M\ O_2$)$^{-1}$ for the aerobic, and 0.003 and 0.0004 $yr^{-1}$ ($\mu M\ SO_4^{2-}$)$^{-1}$ for the anaerobic oxidation of $CH_4$ in the thermocline and the deep water, respectively. These values correspond to 3 months residence time of $CH_4$ for aerobic oxidation at typical $O_2$ concentrations of 200 $\mu$M in the mixolimnion, and to about 20 and 600 years residence time of $CH_4$ for anaerobic oxidation at $SO_4^{2-}$ concentrations present in the thermocline and the deep water, respectively. The effective residence time of $CH_4$ in the deep water in the model is on the order of 100 y, as it is transported upwards by uplift caused by deep water renewal and turbulent diffusion (Figure 6). The vertical structure of simulated oxidation rates agrees well with that of observed abundances of archaea (Figure 2d).

### 3.6. Sensitivity Analysis

[34] The sensitivity of the model in respect to the driving parameters was tested by the following additional simulations. A simulation including seasonal variability was calculated using the following external forcing: sine functions for relative humidity (average 0.75, amplitude 0.15), lake surface temperature (average increasing from 25°C in 1900 to 25.4°C in 1975 and 26°C in 2000, amplitude 2°C), evaporation (average 50 $km^3\ yr^{-1}$, amplitude 7 $km^3\ yr^{-1}$), precipitation (average 35 $km^3\ yr^{-1}$, amplitude 30 $km^3\ yr^{-1}$) and mixolimnion depth (90 m during 20% of the year and 30 m during the other time). Lake surface temperature, precipitation, and humidity exhibit their maxima during the wet season, evaporation and mixing depth during the dry season. We found that effects of seasonality were small on the simulated depth distribution of reactants.

[35] The deep water renewal rate was varied in steps of 10 $km^3\ yr^{-1}$ from 20 to 50 $km^3\ yr^{-1}$. The impact of deep water renewal on concentrations of $CH_4$, $SO_4^{2-}$, $HS^-$, $\delta^{13}CH_4$, and the anaerobic oxidation of $CH_4$, is shown in Figure 7, and on $^3H$ and CFC-12 concentrations in Figure 5. Precipitation and evaporation were varied by ±5 $km^3\ yr^{-1}$, relative humidity by ±10%, and wind speeds of 1 and 6 $m\ s^{-1}$ were simulated. The most significant effects of changes in these parameters could be observed for simulated $^3H$ concentrations due to changes in humidity. A change in relative humidity by 10% resulted in a similar change in simulated $^3H$ concentrations, as if increasing the deep water renewal rate by about 10 $km^3\ yr^{-1}$.

[36] The $\delta^{13}C$ of dissolved $CH_4$ produced in the sediment was varied by ±5‰. This change influenced $\delta^{13}CH_4$ values by the same amount in the whole water column. Fractionation factors were varied by ±0.01 for the aerobic fractionation and by ±0.002 for the anaerobic fractionation of $CH_4$. The former had a significant effect on $\delta^{13}CH_4$ values in the mixolimnion (although this is most probably strongly influenced by shallow sources). The latter caused a variation of about ±0.3‰ in the whole deep water.

[37] The aerobic oxidation rate of $CH_4$ was multiplied and divided by a factor of 10. A higher aerobic oxidation rate would mainly affect concentrations and the $\delta^{13}C$ of dissolved $CH_4$ in the mixolimnion. However, both are most probably strongly influenced by shallow $CH_4$ sources as well as by seasonal fluctuations, and can therefore not be used to calibrate this parameter with high accuracy without further information on shallow $CH_4$ sources.

[38] Finally it was tested whether the observed profiles of $CH_4$, $SO_4^{2-}$, and $HS^-$ could also be reproduced using a model without anaerobic oxidation of methane. In order to achieve this, the following changes had to be made to the model: the diffusivity in the thermocline was increased by a factor of 2 to $2 \times 10^{-5}\ m^2\ s^{-1}$; an additional process was added that reduces $SO_4^{2-}$, and $HS^-$ at approximately the same rate as this is done by the anaerobic oxidation of $CH_4$ in the base model; the $CH_4$ release rate from the sediment was slightly reduced to 0.4 $mmol\ m^{-2}\ yr^{-1}$; the first-order consumption rate of oxygen was increased to 0.5 $yr^{-1}$. With these adaptations of the model, observed $CH_4$ concentrations could be reproduced almost as well as with the base simulation (Figure 8).

## 4. Discussion

[39] In Lake Tanganyika, high concentrations of dissolved $CH_4$ possibly originate from degradation of settling organic particles and 'relict' sediment organic C [*Craig*, 1975; *Hecky*, 1978] under low $SO_4^{2-}$ concentrations (≤25 $\mu$M) as compared to marine systems [*Capone and Kiene*, 1988])

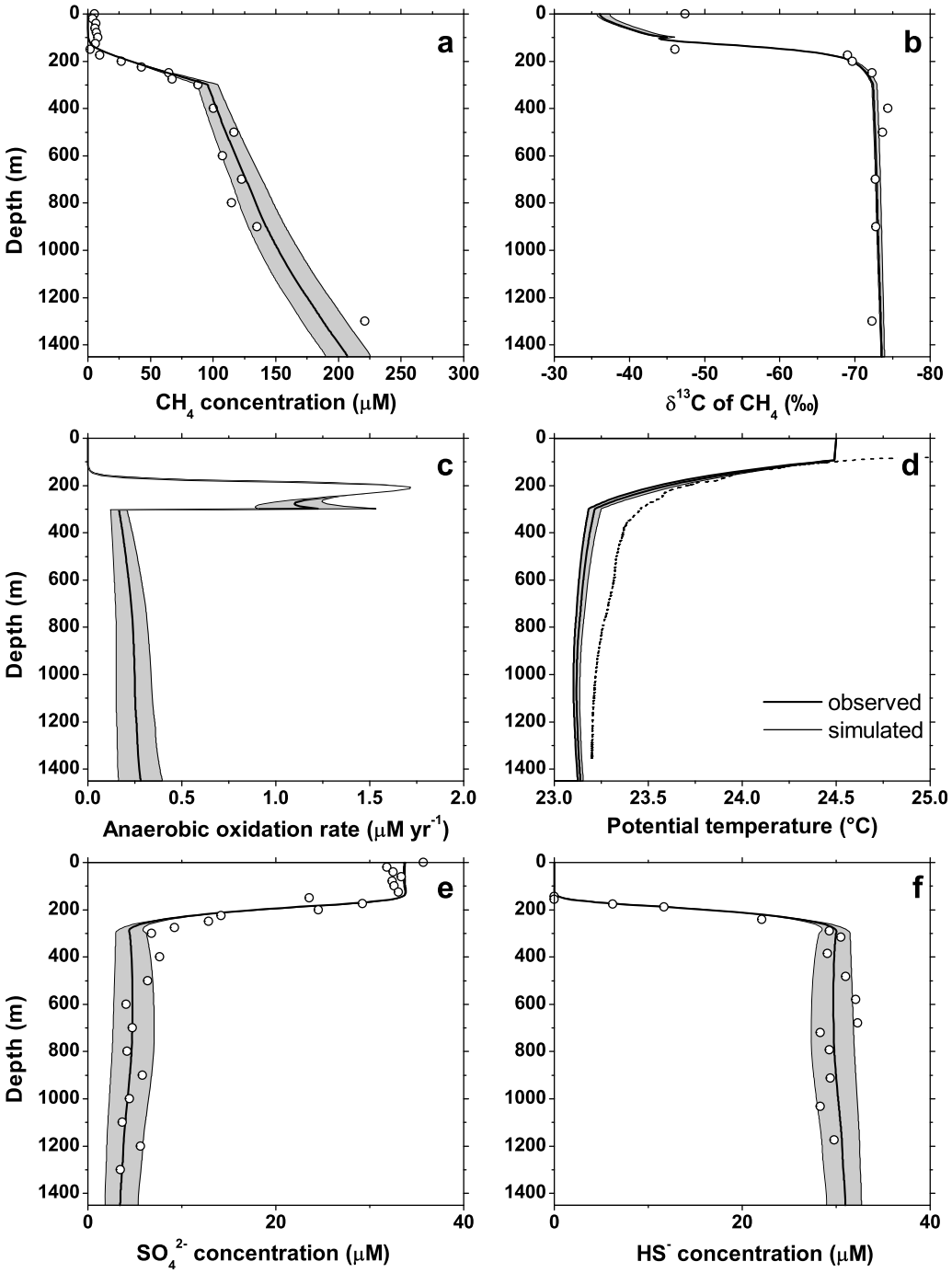


**Figure 7.** Sensitivity of simulated vertical profiles of (a) $CH_4$ concentrations, (b) $\delta^{13}C$ of $CH_4$, (c) the rate of the anaerobic oxidation of $CH_4$, (d) potential temperature, (e) $SO_4^{2-}$, and (f) $HS^-$ concentrations on the deep water renewal rate. The gray bands indicate the range of simulated results for a change of the renewal rate by $\pm 10$ km$^3$ yr$^{-1}$. Open symbols represent measured concentrations, and the dashed line represents the temperature.

(Figures 2a and 2c). According to a recent study by *Alin and Johnson* [2007] this ancient and deep tropical lake stores up to 4 km of sediment, containing a gigantic amount of organic matter, which is partially prone to remineralization at high deep water temperatures [*Sobek et al.*, 2009] as encountered in Lake Tanganyika. The $CH_4$ 'light' C isotopic ratio of −73 ‰ in deep water (Figures 2a and 2c) suggests that it is biologically produced, namely via carbon dioxide ($CO_2$) reduction or fermentation [*Whiticar et al.*, 1986]. Typical $\delta^{13}C$ values produced by both processes in marine and fresh waters are −110 to −55 ‰ for $CO_2$ reduction and −70 to −50 ‰ for fermentation. Although Lake Tanganyika is a tectonic system, contribution of 'light' hydrocarbon gases (−58 to −50 ‰) originating from hydrothermal fluids

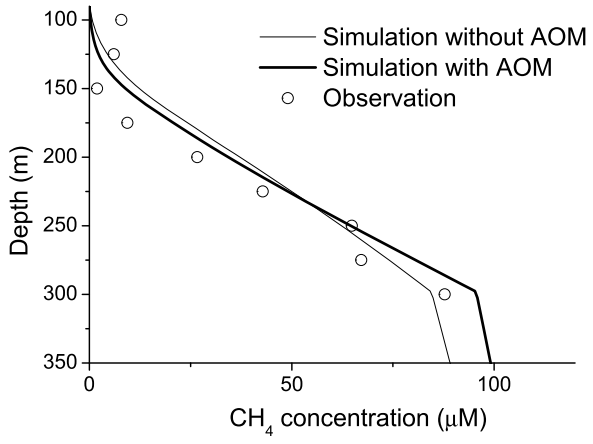


**Figure 8.** Simulated concentrations of $CH_4$ in the thermocline in optimized model versions with and without the anaerobic oxidation of $CH_4$. The differences between the two models are described in section 3.6.

[*Botz and Stoffers*, 1993] did not impact the isotopic signature of water column $CH_4$.

[40] In both basins water column concentrations of dissolved $CH_4$ gradually declined upwards within deep anoxic layers and above in the mixolimnion, while intensely within the fairly narrow thermocline between 90 and 300 m (Figures 2a and 2c). The vertical profiles of $CH_4$ indicate that (1) turbulent diffusion must lead to an upward flux of $CH_4$ from $CH_4$-rich deep water and (2) a sink for $CH_4$ exists at shallower depth compensating the upward flux. Significant vertical gradients in $CH_4$ concentrations were only identified in the anoxic zone, and did not extend into the oxic layer in the southern basin, suggesting that $CH_4$ must be substantially removed in anoxic water. Because of ample $SO_4^{2-}$ concentrations in the stratified water column of Lake Tanganyika, we hypothesize that next to aerobic oxidation the anaerobic oxidation of $CH_4$ may play a role in the elimination of $CH_4$. According to *Rudd* [1980] no oxidative removal of $CH_4$ can be expected below the suboxic zone of Lake Tanganyika. However, one study has demonstrated that the anaerobic oxidation of $CH_4$ may act as a control mechanism of water column concentrations of $CH_4$ in freshwater [*Eller et al.*, 2005]. For this reason, we have evaluated the importance of anaerobic and aerobic methanotrophy for $CH_4$ concentrations in Lake Tanganyika by means of a simplified one-dimensional model.

[41] We found that both in the deep water and in the thermocline, microenvironments geochemically suitable for the anaerobic oxidation of $CH_4$ existed with sufficiently high concentrations of both $SO_4^{2-}$ and $CH_4$ [*Iversen and Jorgensen*, 1985]. $SO_4^{2-}$ is supplied intermittently to the $CH_4$-rich deep water by deep water renewal events, whereas in the thermocline turbulent diffusion supplies $SO_4^{2-}$ from the mixolimnion and $CH_4$ from the deep water. This finding is strongly underscored by simulated rates of the anaerobic oxidation of $CH_4$, and simulated fluxes of $CH_4$, $SO_4^{2-}$, and $HS^-$, which also peaked in this depth range (Figure 2d).

[42] Sulphate is mainly supplied from river inflow [e.g., *Kimbadi et al.*, 1999; *Langenberg et al.*, 2003] and in-lake oxic and anoxic sulfur oxidation between ~150 to 300 m depth, as indicated by the existence of green nonsulphur bacteria in the lake's hypolimnion [*De Wever et al.*, 2005]. Highest downward diffusive fluxes of $SO_4^{2-}$ (~100 mol $s^{-1}$) occurred within the thermocline at ~200 m depth, and matched upward fluxes of $HS^-$ (Figure 9). Hence, we concluded that $HS^-$ concentrations were controlled by $SO_4^{2-}$ reduction. Although thermophilic $SO_4^{2-}$ reduction coupled to oxidation of organic matter was reported from sublacustrine hydrothermal sediments of Lake Tanganyika [*Elsgaard et al.*, 1994], we assumed this process was potentially hampered in these depths due to relatively low $SO_4^{2-}$ concentrations and mutual exclusion by methanogenesis [*Cappenberg*, 1974; *Lovley et al.*, 1982].

[43] The electron acceptor $O_2$, relevant for the aerobic oxidation of $CH_4$ ($CH_4 + 2O_2 \rightarrow CO_2 + 2H_2O$), is mainly supplied from the atmosphere. Oxygen concentrations decreased from 60 m downward and were zero at ~200 m depth in both basins (Figures 2a and 2c). Downward fluxes of oxygen were highly surpassing upward diffusion of $CH_4$, implying that the aerobic oxidation of $CH_4$ can be potentially very high in surface waters (Figures 2d and 9). Hence, aerobic methanotrophy can occur until $O_2$ is depleted to zero, and it is the thermodynamically favorable process in the oxic and upper part of the suboxic zone [*Hazeu*, 1975]. Estimated aerobic oxidations rates peaked at ~140 m depth, exactly where $O_2$ concentrations were already strongly depleted, as was previously described [*Rudd*, 1980; *Reeburgh et al.*, 1991].

[44] According to simulations, ~35 $km^3$ $yr^{-1}$ of water was exchanged by advective processes between the upper 90 m and the deep water below. The estimated deep water renewal rate was similar to the total annual river inflows. However, rivers have been shown to usually stratify at shallow depths and therefore cannot be the major source for this deep water renewal [*Verburg and Hecky*, 2009]. Most probably, density plumes caused by differential cooling of water masses in shallower areas during the dry season are the cause for the deep water exchange. The lowest potential temperature in the vertical profiles was about 23.2°C. The difference in conductivity at 25°C between the surface and the deep water is only about 40–60 $\mu$S $cm^{-1}$, which corresponds to a density difference of <0.03 kg $m^{-3}$. At such high temperatures a difference of ~0.1°C is sufficient to compensate the stabilizing effect of the salinity differences between surface and deep water. Consequently, surface water masses that are cooled below 23°C can plunge to largest depths in Lake Tanganyika. Nearshore temperatures below 23°C were observed in three of four years during a measurement campaign at Mpulungu harbor [*Verburg and Hecky*, 2009]. If the deep water renewal is indeed caused by such density plumes, small differences in the minimum temperature can have a large impact on both the volume and the intrusion depth of these plumes. Therefore, it is expected that the volume of deep water renewal as well as the depths of the resulting intrusions are highly variable from year to year. For example, observations from 1998 indicate the occurrence of a large plume at 400 m depth during the previous year. The estimated deep water renewal rate of ~35 $km^3$ $yr^{-1}$ should be regarded as a long-term average rate. As mentioned above, the sinking water masses transport the oxidants $O_2$ and $SO_4^{2-}$ from the surface layer to deeper waters.

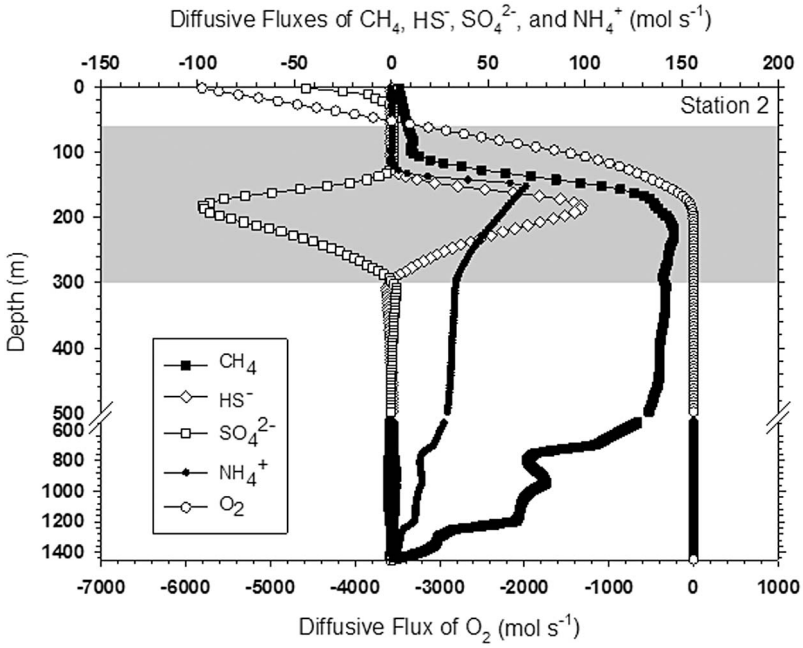


**Figure 9.** Simulated diffusive fluxes (mol s $^{1}$) of $CH_4$, $NH_4^+$, HS , and the electron acceptors $SO_4^2$ and $O_2$ for the anaerobic and aerobic oxidation of $CH_4$ versus depth. Negative values indicate downward and positive values upward fluxes. The thermocline zone is indicated by shading.

[45] The model was able to adequately reproduce measured concentrations of $CH_4$, $O_2$, $SO_4^2$ , and HS in the southern basin (Figure 2c). In the anoxic deep, a net source of 6 g $CH_4$-C m $^{2}$ yr $^{1}$ was required to obtain the observed $CH_4$ concentrations. Furthermore, simulated concentrations of $SO_4^2$ and HS in the thermocline and below ~300 m depth could only be explained by assuming a slow transformation of $SO_4^2$ to HS with a residence time of $SO_4^2$ on the order of 300 years. We propose that the process responsible for this transformation is anaerobic oxidation of $CH_4$. The simulated depth distribution of the aerobic oxidation of $CH_4$ in the whole water column (Figure 2d) revealed highest rates at ~140 m depth under oxic/suboxic conditions, confirming the finding by *Rudd* [1980]. According to the model additional significant $CH_4$ removal is required at ~200 m depth under quasi anoxic conditions suggesting anaerobic $CH_4$ oxidation (Figure 2d). Moreover, the simulations suggested that the anaerobic oxidation of $CH_4$ took place within the whole anoxic deep, even though with a lower rate than in the thermocline. The reaction rate constants were roughly estimated to be 0.02 yr $^{1}$ ($\mu$M $O_2$) $^{1}$ for the aerobic, and to 0.003 yr $^{1}$ ($\mu$M $SO_4^2$ ) $^{1}$ and 0.0004 yr $^{1}$ ($\mu$M $SO_4^2$ ) $^{1}$for the anaerobic elimination of $CH_4$ in the thermocline and the deep water, respectively. Overall, according to the model, anaerobic and aerobic methane oxidation removed each about half of the $CH_4$ released from mineralization in the deep water. The simulated average residence time of $CH_4$ produced below 90 m depth was ~110 years (Figure 6).

[46] In the model, only a few percent of the $CH_4$ produced in the deep water were emitted to the atmosphere. However, simulated $CH_4$ concentrations in the surface layer were only 0.014 $\mu$M, whereas observed concentrations ranged between 0.01 and 10 $\mu$M. Therefore, it must be expected that $CH_4$ emissions to the atmosphere are higher than predicted by the model. A large number of observations would be required to calibrate a model that would aim at reproducing the seasonal variability of surface layer $CH_4$ concentrations, and could therefore give a reliable estimate of emissions to the atmosphere. The available data is insufficient for this purpose. Nevertheless, in order to arrive at an average concentration of 1 $\mu$M in the surface layer, an additional input of about 10 g C-$CH_4$ m $^{2}$ yr $^{1}$ had to be added to the model. Approximately half of this additional input would be oxidized aerobically, the other half would be emitted to the atmosphere. Potential sources of $CH_4$ to the surface layer could be $CH_4$, which is produced in nearshore shallow areas, especially near river inflows, and subsequently distributed horizontally, or $CH_4$ directly introduced by rivers [*Murase et al.*, 2005; *Schmid et al.*, 2007].

[47] The isotopic enrichment of heavy carbon ($^{13}$C) in dissolved $CH_4$ served as an additional valuable evidence for biological $CH_4$ removal [*Barker and Fritz*, 1981; *Reeburgh et al.*, 1991; *Whiticar*, 1999; *Durisch-Kaiser et al.*, 2005] and was compared to model calculations. We observed that microbial oxidation enforced a change in $\delta^{13}CH_4$ along upward $CH_4$ transport. In the narrow zone between 90 to 350 m depth, an isotopic enrichment by on average 23‰ (Figures 2a and 2c) was identified. Mixing processes as a reason for this isotopic imprint can be ruled out due to the lack of sufficient amounts of isotopically heavy $CH_4$ in these shallow depths. Furthermore, changes in $CH_4$ concentrations and in $\delta^{13}CH_4$ did not overlap depthwise (Figures 2a and 2c). This is explained by the low isotope fractionation factor for the anaerobic oxidation of $CH_4$ ($\varepsilon_C$ = 5). A significant change in the C isotope ratio is first observed if ~80% of the $CH_4$ have been oxidized [*Whiticar*, 1999].

[48] Isotopic analyses did not allow for distinguishing between aerobic and anaerobic processes. Hence, to constrain the role of both processes, we detected numerous single archaea and bacteria potentially involved in the oxidation of methane by using FISH [*Pernthaler et al.*, 2002; *Eller et al.*, 2001]. Between 175 and 300 m depth, an enormously elevated abundance of archaea matched with pronounced changes in concentrations of $CH_4$, $\delta^{13}CH_4$, and calculated oxidation rates of $CH_4$ (Figures 2c and 2d). Abundances of ~0.6 to at most 33% archaea of 4′,6′-diamidino-2-phenylindol (DAPI)-stained cells were detected in the thermocline of the northern basin. In the southern basin, highest numbers were located at around 200 m depth, perfectly coinciding with highest calculated rates of the anaerobic oxidation of $CH_4$ (Figure 2d). Archaea were also present in smaller amounts below ~350 m, aligning with simulations that predict anaerobic oxidation of $CH_4$ in the whole water column. We cannot exclude that increased numbers of archaea may also result from an elevated abundance of methanogens. However, the proper correlation ($R = 0.86$, $P < 0.0001$) of archaeal cell counts with simulated rates of the anaerobic oxidation of $CH_4$ suggested a dominant role of archaeal methanotrophs. Methanotrophs of aerobic physiology could also be located using FISH and specific probes for bacterial type I and II methanotrophs [*Eller et al.*, 2001]. Highest abundances (up to 95% type I methanotrophs) occurred close to the top of the suboxic regime, confirming the pattern in calculated aerobic oxidation rates (Figure 2d) and a former study by *Rudd* [1980].

[49] Empirical data and simulations provided several arguments for the assumption that the anaerobic oxidation of $CH_4$ is an important removal process for $CH_4$ in Lake Tanganyika today. First, model calculation allowed identifying a substantial deep water renewal process as a continuous mechanism supplying the electron acceptor $SO_4^{2-}$ to the very deep. Second, between ~150 and 300 m depth downward fluxes of $SO_4^{2-}$ matched upward fluxes of $CH_4$ and HS which is consistent with the anaerobic oxidation of $CH_4$ stoichiometry. Third, the overlap of archaeal numbers with calculated rates of the anaerobic oxidation of $CH_4$ validate the occurrence and importance of the anaerobic oxidation of $CH_4$. In conclusion, the available data support that anaerobic oxidation of $CH_4$ is an important mechanism controlling $CH_4$ removal in the deep water of Lake Tanganyika. Nevertheless, the vertical $CH_4$ profile could also be reproduced with an adapted version of the model without AOM. Ultimate proof of the importance of AOM will therefore require on one hand in situ rate measurements and biomarker analyses, and on the other hand cloning and sequencing of archaea present in the anoxic water column.

[50] It has been speculated that global warming may enforce stratification and that, as a consequence, the anoxic water mass will expand to shallower depths within the upcoming 100 years in Lake Tanganyika [*Verburg et al.*, 2003; *Verburg and Hecky*, 2009; *Cohen et al.*, 2006]. We consider that this change could largely affect the vertical flux of important reactants in the anaerobic oxidation of $CH_4$, at least until the system has reached a new steady state. Hence, meanwhile the anaerobic oxidation of $CH_4$ will stay a major factor restraining $CH_4$ release to the atmosphere, however, over longer time periods an enforced stratification and higher minimal surface temperatures may impede vertical input of $O_2$ and $SO_4^{2-}$ as well as deep water renewal. As a net result $CH_4$ may accumulate below the thermocline.

[51] **Acknowledgments.** We thank the whole crew of the R/V *Maman Benita* for logistical assistance during the research cruises, R. Illi for assisting laboratory analyses, L. Jarc for contributing to the development of the model, E. Deleersnijder for supplying bathymetry data, and two anonymous reviewers for their very helpful comments. This work was supported by internal Eawag funds. Isotopic measurements were possible due to a R'Equip grant from the Swiss National Science Foundation to Carsten J. Schubert.

## References

Aeschbach Hertig, W. (1994), Helium und Tritium als Tracer für physikalische Prozesse in Seen, Ph.D. thesis 10714, 272 pp., ETH, Zürich.

Alin, S. R., and T. C. Johnson (2007), Carbon cycling in large lakes of the world: A synthesis of production, burial, and lake atmosphere exchange estimates, *Global Biogeochem. Cycles*, *21*, GB3002, doi:10.1029/2006GB002881.

Amann, R. I., B. J. Binder, R. J. Olson, S. W. Chisholm, R. Devereux, and D. A. Stahl (1990), Combination of 16S ribosomal RNA targeted oligonuleotide probes with flow cytometry for analyzing mixed microbial populations, *Appl. Environ. Microbiol.*, *56*(6), 1919 1925.

Barker, J. F., and P. Fritz (1981), Carbon isotope fractionation during microbial methane oxidation, *Nature*, *293*(5830), 289 291, doi:10.1038/293289a0.

Bastviken, D., J. Cole, M. Pace, and L. Tranvik (2004), Methane emissions from lakes: Dependence of lake characteristics, two regional assessments, and a global estimate, *Global Biogeochem. Cycles*, *18*, GB4009, doi:10.1029/2004GB002238.

Beal, E. J., C. H. House, and V. J. Orphan (2009), Manganese and iron dependent marine methane oxidation, *Science*, *325*(5937), 184 187, doi:10.1126/science.1169984.

Beyerle, U., W. Aeschbach Hertig, D. M. Imboden, H. Baur, T. Graf, and R. Kipfer (2000), A mass spectrometric system for the analysis of noble gases and tritium from water samples, *Environ. Sci. Technol.*, *34*(10), 2042 2050, doi:10.1021/es990840h.

Boetius, A., K. Ravenschlag, C. J. Schubert, D. Rickert, F. Widdel, A. Gieseke, R. Amann, B. B. Jorgensen, U. Witte, and O. Pfannkuche (2000), A marine microbial consortium apparently mediating anaerobic oxidation of methane, *Nature*, *407*(6804), 623 626, doi:10.1038/35036572.

Bootsma, H. A., and R. E. Hecky (2003), A comparative introduction to the biology and limnology of the African great lakes, *J. Great Lakes Res.*, *29*, 3 18, doi:10.1016/S0380-1330(03)70535-8.

Botz, R. W., and P. Stoffers (1993), Light hydrocarbon gases in Lake Tanganyika hydrothermal fluids (east central Africa), *Chem. Geol.*, *104*(1 4), 217 224, doi:10.1016/0009-2541(93)90152-9.

Branchu, P., and L. Bergonzini (2004), Chloride concentrations in Lake Tanganyika: An indicator of the hydrological budget, *Hydrol. Earth Syst. Sci.*, *8*, 256 265, doi:10.5194/hess-8-256-2004.

Capart, A. (1949), Sondages et carte bathymétrique du lac Tanganyika. Exploration hydrobiologique du lac Tanganyika (1946 47), report, 16 pp., Inst. R. des Sci. Nat. de Belgique, Brussels.

Capone, D. G., and R. P. Kiene (1988), Comparison of microbial dynamics in marine and fresh water sediments Contrasts in anaerobic carbon catabolism, *Limnol. Oceanogr.*, *33*(4), 725 749, doi:10.4319/lo.1988.33.4_part_2.0725.

Cappenberg, T. E. (1974), Interrelations between sulfate reducing and methane producing bacteria in bottom deposits of a freshwater lake. 2. Inhibition experiments, Antonie Van Leeuwenhoek *J. Microbiol.*, *40*(2), 297 306, doi:10.1007/BF00394388.

Cohen, A. S., K. E. Lezzar, J. Cole, D. Dettman, G. S. Ellis, M. E. Gonneea, P. D. Plisnier, V. Langenberg, M. Blaauw, and D. Zilifi (2006), Late Holocene linkages between decade century scale climate variability and productivity at Lake Tanganyika, Africa, *J. Paleolimnol.*, *36*(2), 189 209, doi:10.1007/s10933-006-9004-y.

Cole, J. J., and N. F. Caraco (1998), Atmospheric exchange of carbon dioxide in a low wind oligotorphic lake measured by the addition of SF6, *Limnol. Oceanogr.*, *43*(4), 647 656, doi:10.4319/lo.1998.43.4.0647.

Coulter, G. W., and J. J. Tiercelin (1991), *Lake Tanganyika and its life*, Oxford Univ. Press, London.

Craig, H. (1975), Lake Tanganyika geochemical and hydrolographic study: 1973 expedition, *SIO Ref. Ser.*, *75 5*, 83.

Deuser, W. G., E. T. Degens, G. R. Harvey, and M. Rubin (1973), Methane in Lake Kivu New data bearing on its origin, *Science*, *181*(4094), 51 54, doi:10.1126/science.181.4094.51.

De Wever, A., K. Muylaert, K. Van der Gucht, S. Pirlot, C. Cocquyt, J. P. Descy, P. D. Plisnier, and W. Vyverman (2005), Bacterial community composition in Lake Tanganyika: Vertical and horizontal heterogeneity, *Appl. Environ. Microbiol.*, *71*(9), 5029 5037, doi:10.1128/AEM.71.9.5029-5037.2005.

DEW (2004), *Deutsche Einheitsverfahren zur Wasseruntersuchung*, Wiley VCH, New York.

Durisch Kaiser, E., L. Klauser, B. Wehrli, and C. Schubert (2005), Evidence of intense archaeal and bacterial methanotrophic activity in the Black Sea water column, *Appl. Environ. Microbiol.*, *71*(12), 8099 8106, doi:10.1128/AEM.71.12.8099-8106.2005.

Edmond, J. M., R. F. Stallard, H. Craig, V. Craig, R. F. Weiss, and G. W. Coulter (1993), Nutrient chemistry of the water column of Lake Tanganyika, *Limnol. Oceanogr.*, *38*(4), 725 738, doi:10.4319/lo.1993.38.4.0725.

Eller, G., S. Stubner, and P. Frenzel (2001), Group specific 16S rRNA targeted probes for the detection of type I and type II methanotrophs by fluorescence in situ hybridisation, *FEMS Microbiol. Lett.*, *198*(2), 91 97, doi:10.1111/j.1574-6968.2001.tb10624.x.

Eller, G., L. K. Kanel, and M. Kruger (2005), Cooccurrence of aerobic and anaerobic methane oxidation in the water column of Lake Plusssee, *Appl. Environ. Microbiol.*, *71*(12), 8925 8928, doi:10.1128/AEM.71.12.8925-8928.2005.

Elsgaard, L., D. Prieur, G. M. Mukwaya, and B. B. Jorgensen (1994), Thermophilic sulfate reduction in hydrothermal sediment of Lake Tanganyika, East Africa, *Appl. Environ. Microbiol.*, *60*(5), 1473 1480.

Gourgue, O., E. Deleersnijder, and L. White (2007a), Toward a generic method for studying water renewal, with application to the epilimnion of Lake Tanganyika, *Estuarine Coastal Shelf Sci.*, *74*(4), 628 640, doi:10.1016/j.ecss.2007.05.009.

Gourgue, O., E. Deleersnijder, and L. White (2007b), Toward a generic method for studying water renewal, with application to the epilimnion of Lake Tanganyika, *Estuarine Coastal Shelf Sci.*, *74*, 628 640, doi:10.1016/j.ecss.2007.05.009.

Grasshof, K. (1983), Determination of oxygen, in *Methods of Seawater Analysis*, edited by K. Grasshof, M. Ehrhardt and K. Kremling, pp. 75 89, Verlag Chemie, New York, doi:10.1002/9783527613984.ch4.

Hazeu, W. (1975), Some cultural and physiological aspects of methane utilizing bacteria, Antonie Van Leeuwenhoek *J. Microbiol.*, *41*(1), 121 134, doi:10.1007/BF02565044.

Hecky, R. E. (1978), The Kivu Tanganyika basin the last 14,000 years, *Pol. Arch. Hydrobiol.*, *25*, 159 165.

Hecky, R. E. (1991), The pelagic ecosystem, in *Lake Tanganyika and Its Life*, edited by G. W. Coulter et al., pp. 90 110, Oxford Univ. Press, Oxford.

Hofer, M., and D. M. Imboden (1998), Simultaneous determination of CFC 11, CFC 12, N 2 and Ar in water, *Anal. Chem.*, *70*(4), 724 729, doi:10.1021/ac970499o.

Imboden, D. M., R. F. Weiss, H. Craig, R. L. Michel, and C. R. Goldman (1977), Lake Tahoe geochemical study. 1. Lake chemistry and tritium mixing study, *Limnol. Oceanogr.*, *22*, 1039 1051, doi:10.4319/lo.1977.22.6.1039.

International Atomic Energy Agency/World Meteorological Organization (2006), Global Network of Isotopes in Precipitation. The GNIP Database, accessible at http://www naweb.iaea.org/napc/ih/IHS_resources_gnip.html.

International Panel on Climate Control (2007), *Climate Change 2007:* 4th *Assessment Report*, Cambridge Univ. Press, New York.

Iversen, N., and B. B. Jorgensen (1985), Anaerobic methane oxidation rates at the sulfate methane transition in marine sediments from Kattegat and Skagerrak (Denmark), *Limnol. Oceanogr.*, *30*(5), 944 955, doi:10.4319/lo.1985.30.5.0944.

Järvinen, M., K. Salonen, J. Sarvala, K. Vuorio, and A. Virtanen (1999), The stoichiometry of particulate nutrients in Lake Tanganyika Implications for nutrient limitation of phytoplankton, *Hydrobiologia*, *407*, 81 88, doi:10.1023/A:1003706002126.

Kimbadi, S., A. Vandelannoote, H. Deelstra, M. Mbemba, and F. Ollevier (1999), Chemical composition of the small rivers of the north western part of Lake Tanganyika, *Hydrobiologia*, *407*, 75 80, doi:10.1023/A:1003749817147.

Knox, M., P. D. Quay, and D. Wilbur (1992), Kinetic isotopic fractionation during air water gas transfer of $O_2$, $N_2$, $CH_4$, and $H_2$, *J. Geophys. Res.*, *97*, 20,335 20,343, doi:10.1029/92JC00949.

Langenberg, V. T., S. Nyamushahu, R. Roijackers, and A. A. Koelmans (2003), External nutrient sources for Lake Tanganyika, *J. Great Lakes Res.*, *29*, 169 180, doi:10.1016/S0380-1330(03)70546-2.

Lucas, L. L., and M. P. Unterweger (2000), Comprehensive review and critical evaluation of the half life of tritium, *J. Res. Natl. Inst. Stand. Technol.*, *105*, 541 549.

Lovley, D. R., D. F. Dwyer, and M. J. Klug (1982), Kinetic analysis of competition between sulfate reducers and methanogens for hydrogen in sediments, *Appl. Environ. Microbiol.*, *43*(6), 1373 1379.

Matzinger, A., M. Schmid, E. Veljanoska Sarafiloska, S. Patceva, D. Guseska, B. Wagner, B. Müller, M. Sturm, and A. Wüest (2007), Eutrophication of ancient Lake Ohrid Global warming amplifies detrimental effects of increased nutrient inputs, *Limnol. Oceanogr.*, *52*(1), 338 353, doi:10.4319/lo.2007.52.1.0338.

Murase, J., Y. Sakai, A. Kametani, and A. Sugimoto (2005), Dynamics of methane in mesotrophic Lake Biwa, Japan, *Ecol. Res.*, *20*, 377 385, doi:10.1007/s11284-005-0053-x.

Michaelis, W., et al. (2002), Microbial reefs in the Black Sea fueled by anaerobic oxidation of methane, *Science*, *297*(5583), 1013 1015, doi:10.1126/science.1072502.

Naithani, J., F. Darchambeau, E. Deleersnijder, J. P. Descy, and E. Wolanski (2007), Study of the nutrient and plankton dynamics in Lake Tanganyika using a reduced gravity model, *Ecol. Modell.*, *200*(1 2), 225 233, doi:10.1016/j.ecolmodel.2006.07.035.

Nicholson, S. E., and X. Yin (2004), Mesoscale patterns of rainfall, cloudiness and evaporation over the great lakes of East Africa, in *The East African Great Lakes: Limnology, Palaeolimnology and Biodiversity*, edited by E. O. Odada and D. O. Olago, *Adv. Global Change Res.*, *12*(2), 93 119, doi:10.1007/0-306-48201-0_3.

Omlin, M., P. Reichert, and R. Forster (2001), Biogeochemical model of Lake Zürich: Model equations and results, *Ecol. Modell.*, *141*, 77 103, doi:10.1016/S0304-3800(01)00256-3.

O'Reilly, C. M., S. R. Alin, P. D. Plisnier, A. S. Cohen, and B. A. McKee (2003), Climate change decreases aquatic ecosystem productivity of Lake Tanganyika, Africa, *Nature*, *424*, 766 768, doi:10.1038/nature01833.

Panganiban, A. T., T. E. Patt, W. Hart, and R. S. Hanson (1979), Oxidation of methane in the absence of oxygen in lake water samples, *Appl. Environ. Microbiol.*, *37*(2), 303 309.

Pasche, N., G. Alunga, K. Mills, F. Muvundja, D. B. Ryves, M. Schurter, B. Wehrli, and M. Schmid (2010), Abrupt onset of carbonate deposition in Lake Kivu during the 1960s: Response to recent environmental changes, *J. Paleolimnol.*, *44*, 931 946, doi:10.1007/s10933-010-9465-x.

Peeters, F., R. Kipfer, M. Hofer, D. M. Imboden, and V. M. Domysheva (2000), Correction to "Vertical turbulent diffusion and upwelling in Lake Baikal estimated by inverse modeling of transient tracers" by F. Peeters, R. Kipfer, M. Hofer, D. M. Imboden, and V. M. Domysheva, *J. Geophys. Res.*, *105*(C6), 14,283, doi:10.1029/2000JC000367.

Peeters, F., D. Finger, M. Hofer, M. Brennwald, D. M. Livingstone, and R. Kipfer (2003), Deep water renewal in Lake Issyk Kul driven by differential cooling, *Limnol. Oceanogr.*, *48*, 1419 1431, doi:10.4319/lo.2003.48.4.1419.

Pernthaler, A., J. Pernthaler, and R. Amann (2002), Fluorescence in situ hybridization and catalyzed reporter deposition for the identification of marine bacteria, *Appl. Environ. Microbiol.*, *68*(6), 3094 3101, doi:10.1128/AEM.68.6.3094-3101.2002.

Petzold, L. (1983), A description of DASSL: A differential/algebraic system solver, in *Scientific Computing: Applications of Mathematics and Computing to the Physical Sciences*, edited by R. Stepleman, pp. 65 68, North Holland, Amsterdam.

Pilskaln, C. H. (2004), Seasonal and interannual particle export in an African rift valley lake: A 5 yr record from Lake Malawi, southern East Africa, *Limnol. Oceanogr.*, *49*(4), 964 977, doi:10.4319/lo.2004.49.4.0964.

Podsetchine, V., T. Huttula, and H. Savijärvi (1999), A three dimensional circulation model of Lake Tanganyika, *Hydrobiologia*, *407*, 25 35, doi:10.1023/A:1003758003034.

Pollack, H. N., S. J. Hurter, and J. R. Johnson (1993), Heat flow from the Earth's interior: Analysis of the global data set, *Rev. Geophys.*, *31*, 267 280, doi:10.1029/93RG01249.

Porter, K. G., and Y. S. Feig (1980), The use of Dapi for identifying and counting aquatic microflora, *Limnol. Oceanogr.*, *25*(5), 943 948, doi:10.4319/lo.1980.25.5.0943.

Raghoebarsing, A. A., et al. (2006), A microbial consortium couples anaerobic methane oxidation to denitrification, *Nature*, *440*(7086), 918 921, doi:10.1038/nature04617.

Ramlal, P. S., R. E. Hecky, H. A. Bootsma, S. L. Schiff, and M. J. Kingdon (2003), Sources and fluxes of organic carbon in Lake Malawi/Nyasa, *J. Great Lakes Res.*, *29*, Suppl. 2, 107 120, doi:10.1016/S0380-1330(03)70542-5.

Reeburgh, W. S., B. B. Ward, S. C. Whalen, K. A. Sandbeck, K. A. Kilpatrick, and L. J. Kerkhof (1991), Black Sea methane geochemistry, *Deep Sea Res., Part A*, *38*, S1189 S1210, doi:10.1016/S0198-0149(10)80030-5.

Reichert, P. (1994), AQUASIM A tool for simulation and data analysis of aquatic systems, *Water Sci. Technol.*, *30*(2), 21 30.

Reichert, P. (1998), AQUASIM 2.0 User Manual, 214 pp., Eawag, Dübendorf, Switzerland.

Rudd, J. W. M. (1980), Methane oxidation in Lake Tanganyika (East Africa), *Limnol. Oceanogr.*, *25*(5), 958 963, doi:10.4319/lo.1980.25.5.0958.

Schmid, M., M. Halbwachs, B. Wehrli, and A. Wuest (2005), Weak mixing in Lake Kivu: New insights indicate increasing risk of uncontrolled gas eruption, *Geochem. Geophys. Geosyst.*, *6*, Q07009, doi:10.1029/2004GC000892.

Schmid, M., M. Halbwachs, and A. Wüest (2006), Simulation of $CO_2$ concentrations, temperature, and stratification in Lake Nyos for different degassing scenarios, *Geochem. Geophys. Geosyst.*, *7*, Q06019, doi:10.1029/2005GC001164.

Schmid, M., M. De Batist, N. Granin, V. A. Kapitanov, D. F. McGinnis, I. B. Mizandrontsev, A. I. Obzhirov, and A. Wüest (2007), Sources and sinks of methane in Lake Baikal A synthesis of measurements and modeling, *Limnol. Oceanogr.*, *52*, 1824 1837, doi:10.4319/lo.2007.52.5.1824.

Schubert, C. J., et al. (2006), Aerobic and anaerobic methanotrophs in the Black Sea water column, *Environ. Microbiol.*, *8*(10), 1844 1856, doi:10.1111/j.1462-2920.2006.01079.x.

Smemo, K. A., and J. B. Yavitt (2007), Evidence for anaerobic $CH_4$ oxidation in freshwater peatlands, *Geomicrobiol. J.*, *24*(7), 583 597, doi:10.1080/01490450701672083.

Sobek, S., E. Durisch Kaiser, R. Zurbrügg, N. Wongfun, M. Wessels, N. Pasche, and B. Wehrli (2009), Organic carbon burial efficiency in lake sediments controlled by oxygen exposure time and sediment source, *Limnol. Oceanogr.*, *54*(6), 2243 2254, doi:10.4319/lo.2009.54.6.2243.

Spigel, R. H., and G. W. Coulter (1996), Comparison of hydrology and physical limnology of the East African great lakes: Tanganyika, Malawi, Victoria, Kivu and Turkana (with reference to some North American Great Lakes), in *The Limnology, Climatology and Paleoclimatology of the East African Lakes*, edited by T. C. Johnson and E. O. Odada, pp. 103 139, Gordon and Breach, Toronto, Ont., Canada.

Stappers, L. (1913), *The Stappers Survey, 1911 1913, Hydrographical and biological exploration of Lake Tanganyika and Lake Moero*, Vromant, Brussels.

Stenuite, S., S. Pirlot, M. A. Hardy, H. Sarmento, A. L. Tarbe, B. Leporcq, and J. P. Descy (2007), Phytoplankton production and growth rate in Lake Tanganyika: Evidence of a decline in primary productivity in recent decades, *Freshwater Biol.*, *52*, 2226 2239, doi:10.1111/j.1365-2427.2007.01829.x.

Stevens, C. M., and M. Wahlen (2000), The isotopic composition of atmospheric methane and its sources, in *Atmospheric Methane*, edited by M. A. K. Khalil, pp. 25 41, Springer, Berlin.

Strous, M., and M. S. M. Jetten (2004), Anaerobic oxidation of methane and ammonium, *Annu. Rev. Microbiol.*, *58*, 99 117, doi:10.1146/annurev.micro.58.030603.123605.

Tiercelin, J. J., et al. (1993), Hydrothermal vents in Lake Tanganyika, East African Rift system, *Geology*, *21*, 499 502, doi:10.1130/0091-7613(1993)021<0499:HVILTE>2.3.CO;2.

Valentine, D. L., and W. S. Reeburgh (2000), New perspectives on anaerobic methane oxidation, *Environ. Microbiol.*, *2*(5), 477 484, doi:10.1046/j.1462-2920.2000.00135.x.

Van der Nat, F. J., and J. J. Middelburg (2000), Methane emission from tidal freshwater marshes, *Biogeochemistry*, *49*(2), 103 121, doi:10.1023/A:1006333225100.

Verburg, P., and R. E. Hecky (2009), The physics of the warming of Lake Tanganyika by climate change, *Limnol. Oceanogr.*, *54*(6_part_2), 2418 2430, doi:10.4319/lo.2009.54.6_part_2.2418.

Verburg, P., R. E. Hecky, and H. Kling (2003), Ecological consequences of a century of warming in Lake Tanganyika, *Science*, *301*(5632), 505 507, doi:10.1126/science.1084846.

Walker, S. J., R. F. Weiss, and P. K. Salameh (2000), Reconstructed histories of the annual mean atmospheric mole fractions for the halocarbons CFC 11, CFC 12, CFC 113, and carbon tetrachloride, *J. Geophys. Res.*, *105*(C6), 14,285 14,296, doi:10.1029/1999JC900273.

Wang, Y., and P. Van Cappellen (1996), A multicomponent reactive transport model of early diagenesis: Application to redox cycling in coastal marine sediments, *Geochim. Cosmochim. Acta*, *60*, 2993 3014, doi:10.1016/0016-7037(96)00140-8.

Wanninkhof, R. (1992), Relationship between gas exchange and wind speed over the ocean, *J. Geophys. Res.*, *97*, 7373 7382, doi:10.1029/92JC00188.

Warner, M. J., and R. F. Weiss (1985), Solubilities of chlorofluorocarbons 11 and 12 in water and seawater, *Deep Sea Res., Part A*, *32*(12), 1485 1497, doi:10.1016/0198-0149(85)90099-8.

Whiticar, M. J. (1999), Carbon and hydrogen isotope systematics of bacterial formation and oxidation of methane, *Chem. Geol.*, *161*, 291 314, doi:10.1016/S0009-2541(99)00092-3.

Whiticar, M. J., E. Faber, and M. Schoell (1986), Biogenic methane formation in marine and fresh water environments $CO_2$ reduction vs acetate fermentation isotope evidence, *Geochim. Cosmochim. Acta*, *50*(5), 693 709, doi:10.1016/0016-7037(86)90346-7.

Wüest, A., G. Piepke, and D. C. Van Senden (2000), Turbulent kinetic energy balance as a tool for estimating vertical diffusivity in wind forced stratified waters, *Limnol. Oceanogr.*, *45*, 1388 1400, doi:10.4319/lo.2000.45.6.1388.

T. Diem, C. Dinkel, M. Schmid, C. J. Schubert, and B. Wehrli, Eawag, Swiss Federal Institute of Aquatic Science and Technology, CH 6047 Kastanienbaum, Switzerland.

E. Durisch Kaiser, Institute of Biogeochemistry and Pollutant Dynamics, ETH, CH 8092 Zurich, Switzerland. (edith.durisch kaiser@env.ethz.ch)

R. Kipfer, Eawag, Swiss Federal Institute of Aquatic Science and Technology, CH 8600 Dübendorf, Switzerland.

F. Peeters, Limnological Institute, Department of Biology, University of Konstanz, D 78464 Konstanz, Germany.